.Synthesis and Characterization of Near Infrared Absorbing Styryl-Bodipy for Efficient Energy Transfer to Squaraine Dyes

Vinita Kumari

A dissertation submitted for the partial fulfilment

of BS-MS dual degree in Science

CERTIFICATE OF EXAMINATION

This is to certify that the dissertation titled "**Synthesis and Characterization of Near Infrared   Absorbing Styryl-Bodipy for Efficient Energy Transfer to Squaraine Dyes**" submitted by Ms. Vinita Kumari. (Reg. No. MS14144) for the partial fulfillment of BS-MS dual degree programme of the Institute, has been examined by the thesis committee duly appointed by the Institute. The committee finds the work done by the candidate satisfactory and recommends that the report be accepted.

Dr. Sugumar Venkataramani   **Dr. Raj Kumar Roy**   **Dr. Sanchita Sengupta**

Assistant Professor   Assistant Professor   Assistant Professor

IISER Mohali   IISER Mohali   IISER Mohali

(Supervisor)

Dated :

DECLARATION

The work presented in this dissertation has been carried out by me under the guidance of **Dr. Sanchita Sengupta** at the **Indian Institute of Science Education and Research, Mohali.**

This work has not been submitted in part or in full for a degree, a diploma, or a fellowship to any other university or institute. Whenever contributions of others are involved, every effort is made to indicate this clearly, with due acknowledgement of collaborative research and discussions. This thesis is a bonafide record of original work done by me and all sources listed within have been detailed in the bibliography.

Vinita Kumari

(Candidate)

Dated:

In my capacity as the supervisor of the candidate's project work, I certify that the above statements by the candidate are true to the best of my knowledge.

Dr. Sanchita Sengupta

(Supervisor)

ACKNOWLEDGEMENT

Contents

List of Figures

Figure 2.14. (a). Spectral overlap of compound **6a** emission and **NIRSQ** absorption.

(b). Emission spectra (excite at 425 nm) of compound 4a (21 μM)-only (red), and 4a (21 μM)/SQ2 co-solutions in chloroform.

List of Tables

List of Scheme

List of Abbreviations

BODIPY   -   Boradiazaindacene

TFA   -   Trifluoroacetic acid

DCM   -   Dichloromethane

THF   -   Tetrahydrofuran

DIPA   -   Diisopropyl amine

DMF   -   Dimethylformamide

NIS   -   N-Iodosuccinimide

SQ   -   Squaraine

$CHCl_3$ -   Chloroform

$CDCl_3$ -   Deuterated chloroform

DIPEA   -   Diisopropylethylamine

K_2CO_3 -   Potassium Carbonate

$NaHCO_3$ -   Sodium Bicarbonate

Na_2SO_4 -   Sodium Sulphate

CuI   -   Copper Iodide

PE   -   Petroleum Ether

RT   -   Room Temperature

FRET   -   Förster Resonance Energy Transfer

TLC   -   Thin layer chromatography

NMR   -   Nuclear magnetic resonance

UV-Vis	-	Ultraviolet Visible
NIR	-	Near Infrared
Eq	-	Equivalent
nm	-	Nanometer
mM	-	Millimolar
ESI-TOF	-	Electospray Ionization Time of flight
HRMS	-	High Resolution Mass Spectrometry
^{1}H-NMR	-	Proton NMR
^{13}C-NMR	-	Carbon-13 NMR

Abstract

 NIR absorbing and emitting bodipy dyes have been synthesized that are functionalized with styryl moieties containing solubility inducing hexyl and ethylhexyl chains and monofunctionalization at the C-5-position. NIR styryl BODIPY dyes containing iodo-substituent at C-5 position **3a-5a** and **3b-5b** were synthesized by Knoevenagel Condensation reaction, Corresponding TMS functionalized compounds **4a-6a** and **4b-6b** were synthesized by Sonogashira reaction and all the synthesized compounds were characterized by ^{1}H NMR, ^{13}C NMR, mass spectrometry, UV-vis absorption and fluorescence studies. These BODIPY dyes form suitable Förster Resonance Energy Transfer (FRET) pairs with squaraine dyes. Energy transfer efficiencies (ETE) for the four FRET pairs (styrylBODIPY and suitable squaraine dyes **SQ2**, **SQ4**, **NIRSQ**) were examined by integrated area under the emission intensity curve analysis of the pure donor emission as well as the emission of donor in the presence of acceptors (i.e., in co-solutions). Among these four FRET pairs, **4a**+**SQ2** showed highest ETE of ~ 68 %, other FRET pairs showed ETE of ~ 52-55 %. Such styryl BODIPY compounds have potential applications in bio-labelling and bio- imaging studies which will be explored by us in the future.

CHAPTER-1

Introduction

1.1. Energy Transfer Mechanism

Energy Transfer is an important photophysical process relevant in natural photosynthesis, organic solar cells, biological imaging purposes, and in several other (opto)electronic applications[1]. A photon is emitted by an energy donor molecule and is absorbed by an acceptor molecule in radiative transfer mechanism, whereas a nonradiative transfer occurs without the emission of a real photon (virtual photon) as any electromagnetic interaction. Energy transfer happens in two ways namely, heterotransfer and homotransfer[2].

$$D^* + D \longrightarrow D + D^*$$
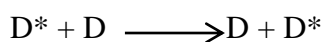
D* is the excited state energy donor and if energy donor and acceptor are identical molecules, then it is called Homotransfer.

$$D^* + A \longrightarrow D + A^*$$
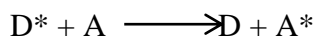
If energy donor (D) and acceptor (A) are different than it is termed as Heterotransfer.

The average distance between donor and acceptor molecule is larger than the wavelength in the radiative energy transfer. Donor absorbs the energy at shorter wavelength whereas the acceptor absorbs at longer wavelength. The cases where the distance between donor and acceptor is below 1 nm, intermolecular or intramolecular collision happens, whereas a distance is higher than 10 nm than photon emission is dominant. The nonradiative energy transfer usually happens in two pathways: through bond (Dexter type energy transfer), through space (Förster Resonance Energy Transfer (FRET)). For nonradiative energy transfer there are two interactions, Coulombic interactions and Intermolecular orbital overlap. The Coulombic interaction consists of short range multipolar interactions and long range dipole-dipole interactions (Förster type). The intermolecular orbital overlap interaction consists of electron exchange (Dexter type) and charge resonance interactions. For coulombic

interactions there can be possibility of singlet-singlet energy transfer, and for intermolecular orbital overlap triplet-triplet energy transfer can occur[2].
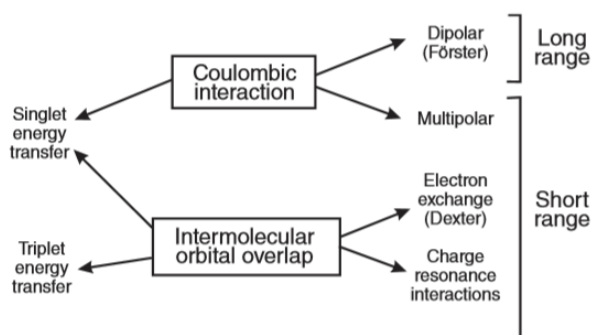
Figure 1.1. Types of nonradiative energy transfer mechanism. (Courtesy: Molecular Fluorescence: Principles and Application, by Bernard Valeur and Mário Nuno Berberan-Santos)

1.1.1. Förster Resonance Energy Transfer (FRET)

Förster Resonance Energy Transfer (FRET) is a collision free process where non-radiative transfer of energy occurs from excited state donor to ground state acceptor through long range dipole-dipole interactions, based on point dipole approximation. Energy transfer happens in FRET is through space and therefore, no direct conjugation is needed between the energy donor and the energy acceptor parts. FRET is a distance dependent photophysical process[1]. Energy transfer between two molecules through space in FRET mechanism is considered as oscillating electric dipoles in the classical model. Initially, upon photoexcitation, the donor dipole is in oscillation in the excited state, and the acceptor's dipole is at rest in the ground state. The nonradiative transfer by dipole-dipole interaction is possible at distances up to nearly ~10 nm. FRET occurs in the range of 1-10 nm. Upon photoexcitation, electron is excited in the donor (D*) in LUMO level and this corresponds to an oscillating dipole. When an acceptor molecule with suitable spectral overlap (i.e., donor emission and acceptor absorption overlap) is available, the excitation energy is transferred to the acceptor molecule. This happens by the oscillating donor dipole coming back to ground state and in the process transfers its energy to the acceptor ground state electron which is then excited and starts oscillating. This is the reason that FRET is considered as a dipole-dipole interaction where the excited electrons are considered as oscillating dipoles as discussed above.

(a)

(b)
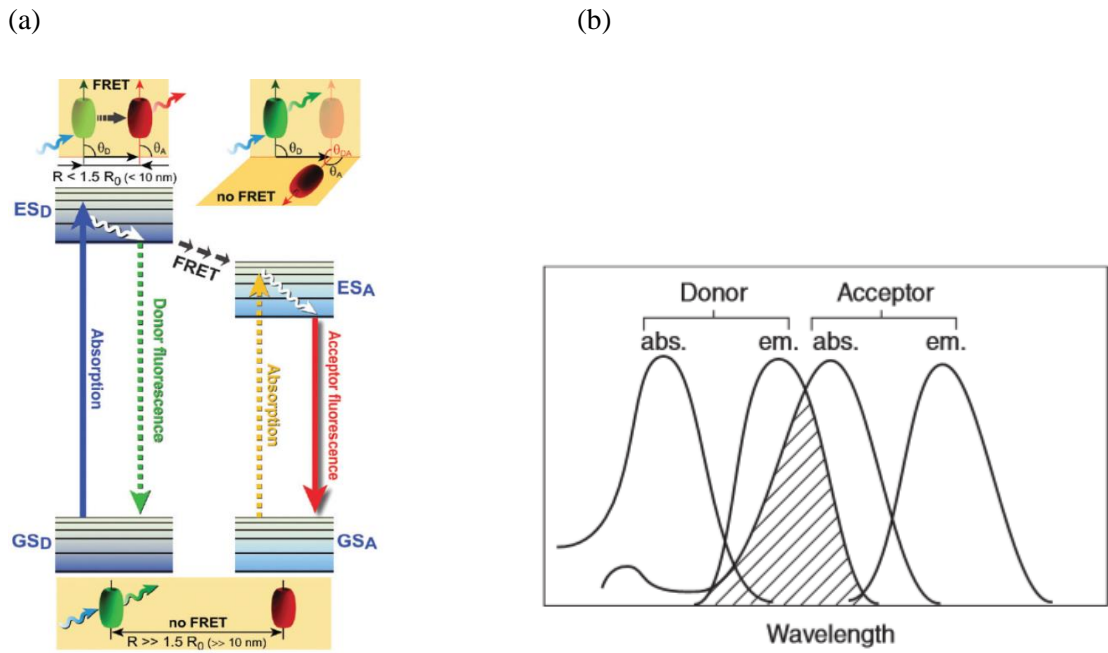
Figure 1.2. (a). Energy level diagram of donor and acceptor molecule. (b). Spectal overlap diagram of donor emission and acceptor absorption. (Courtesy: Molecular Fluorescence: Principles and Application by Bernard Valeur and Mário Nuno Berberan-Santos)

Förster theory states that the rate of energy transfer depends on spectral overlap of the emission of the energy donor molecule with the absorption of the energy acceptor molecule, depends upon the distance between the donor and acceptor molecules, and also upon the orientation of donor and acceptor molecule transition dipole moments. Trnaisiton dipole is the dipole moment associated with a transition that happens from S_0 to S_1 state in any molecule upon photoexcitation. Moreover, for FRET it is necessary that band gap of energy acceptor should be smaller than the energy donor so that the excitation energy of the energy donor can be transferred easily to the energy acceptor. The spectral overlap integral is given by the following equation 1:

Spectral Overlap Integral (1)

$$J(\lambda) = \frac{\int_0^\infty I_D(\lambda)\varepsilon_A(\lambda)\lambda^4 d\lambda}{\int_0^\infty I_D(\lambda)d\lambda}$$

where, $I_D(\lambda)$ is the emission intensity of donor at a particular wavelength λ, $\varepsilon_A(\lambda)$ is the extinction coefficient of the acceptor at a particular wavelength λ.

Förster Radius is the distance between energy donor and energy acceptor at which 50 % of the excitation energy is transferred from the donor to the acceptor. Förster Radius is typically in the range of 1-10 nm[1] and is given by equation 2.

Förster Radius (2)

$$R_0 = 0.211 \frac{\kappa^2 \phi_D J(\lambda)}{n^4}$$
(in Å)

where, κ^2 is the orientation factor of the transition dipoles between donor and acceptor and is usually considered a value of 2/3 for most FRET pairs, ϕ_D is the fluorescence quantum yield of donor in the absence of acceptor, $J(\lambda)$ is the spectral overlap integral of the donor emission and the acceptor absorption and n is the refractive index of the medium (solvent) of energy transfer. The rate of energy transfer is given by equation 3:

Rate of Energy Transfer (3)

$$k_{ET} = \frac{1}{\tau_D} \left(\frac{R_0}{R} \right)^6$$

where, R_0 is the Förster Radius which can be calculated, τ_D is the lifetime of donor molecule in the absence of acceptor, R is the center to center distance of the donor and acceptor transition dipoles.

The extent of energy transfer is dependent on the fluorescence intensities of donor in absence and presence of acceptors or their fluorescence lifetimes and is given by the equation 4:

Energy Transfer Efficiency (4)

$$E = 1 - \frac{F_{DA}}{F_D} \qquad E = 1 - \frac{\tau_{DA}}{\tau_D}$$

Where, F_{DA} is the integrated area under the curve of fluorescence intensity of donor emission in the presence of acceptor molecule, F_D is the integrated area under the curve of fluorescence intensity of donor emission in the absence of acceptor, τ_{DA} is the lifetime of donor in the presence of acceptor, τ_D is the lifetime of donor molecule.
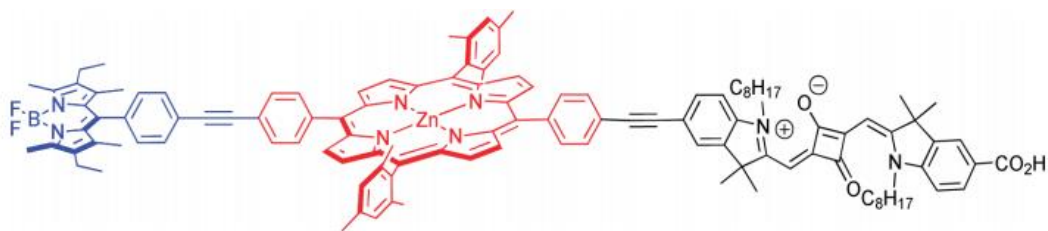
Figure 1.3. Example of FRET based energy transfer cassettes (Coupled system) [3]

Courtesy: (J. Warnan, F. Buchet, Y. Pellegrin, E. Blart, F. Odobel *Org. Lett.* **2011**, 3944–3947)

The trichromophoric sensitizer, covalently connected with boradiazaindacene (BODIPY), zinc porphyrin (ZnP), and squaraine (SQ) units. There is increase in power conversion efficiency by 25 %.
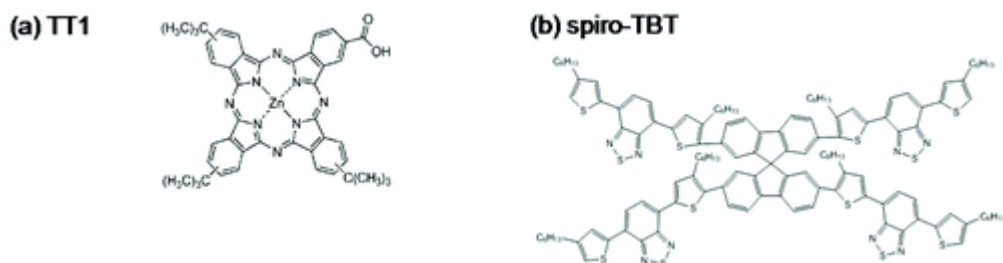
Figure 1.4. Example of FRET based energy transfer cassettes (Physical mixing system) [4]. Courtesy: (*Nano Lett.* 2010, 10, 4981—4988)

Spiro-linked molecule (spiro-OMeTAD) acts as a secondary absorber in solid state excitonic solar cells, blend with TT1 dye [5]. They show increase in power conversion efficiency was 16.5 %. They observed the excitation energy transfer was 21.5 %.

1.2. BODIPY Dyes as possible Energy Donor

1.2.1. BODIPY dyes

4,4-Difluoro-4-bora-3a,4a-diaza-s-indacene (abbreviated as BODIPY) dyes were first discovered in 1968 by Treibs and Kreuzer. In recent decades these small molecule dyes have been popularly used because of their exceptional photophysical properties. BODIPY dyes show strong UV absorption and emit sharp fluorescence with near unity quantum yields. These dyes are stable and dissolve in organic solvents by changing their structure. Another property is that usually these dyes are relatively insensitive to polarity and pH of their environment. These dyes are widely used in biology for labelling of protein and

DNA[6], because their structures can be easily tuned for such biomolecular recognition. Owing to their structural versatility and therefore, color tunability, these dyes are used extensively in artificial light harvesting systems[7], biological imaging[8] and chemosensors[9].

BODIPY molecules can be easily functionalized by coupling and condensation reactions. These molecules usually absorb and emit in the spectral green region (500-550 nm) and very are usually not soluble in water. However, they can be functionalized with water soluble side chains such as oligoethylene glycol chains[10] and so on. Therefore, by suitable chemical modification in the BODIPY structures, they can be designed for using them more efficiently in the imaging in living cells or whole organisms[5]. The IUPAC numbering of BODIPY and dipyrromethenes are different. Here α, β and meso terms are used to indicate the same positions (Figure 1.5).
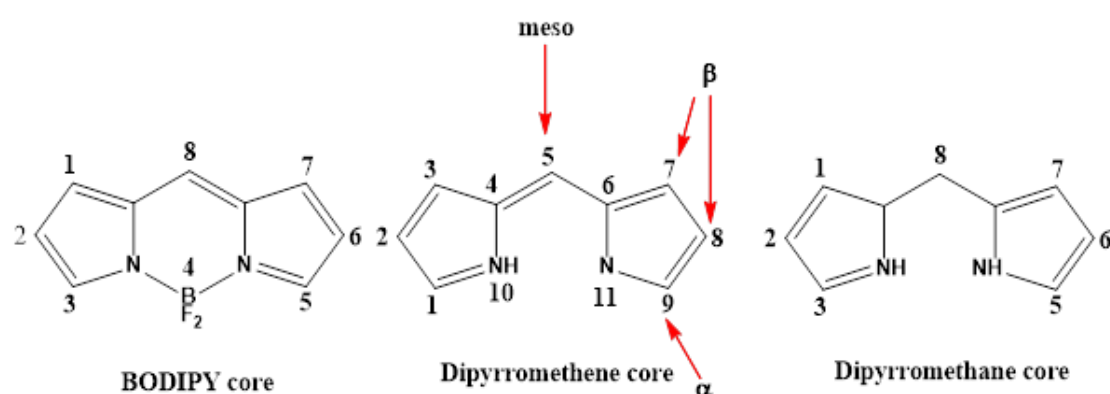
Figure 1.5. Numbering System of BODIPY Dipyrromethene, Dipyrromethane[9]

The unsubstituted BODIPY has a absorption around 500 nm. 8th position in BODIPY core is called meso position. Addition of aromatic rings and groups from meso position does not cause a significant change in the photophysical properties because any extension in this position leads to crossed conjugation rather than extended conjugation. The C-1, C-7 positions on the BODIPY substituted with methyl group prevent the free rotation of the phenyl group on the meso position and thereby reduce the loss of energy from excited state via non-irradiative decay. Substitution on ortho position of phenyl group gives high quantum yields because of the same reason that ortho substituents leads to restricted rotation and thus reduced the non-radiative decay pathways (Figure 1.6). The C-1, C-3, C-5 and C-7 positions on BODIPY can be substituted with suitable functional groups or aryl groups using condensation reactions or coupling reactions and usually such reactions

are of reasonably good yields. Moreover, such compounds because of extended π-conjugation show red shifted absorption and emission spectra with respect to the core-unsusbtituted BODIPY[9].
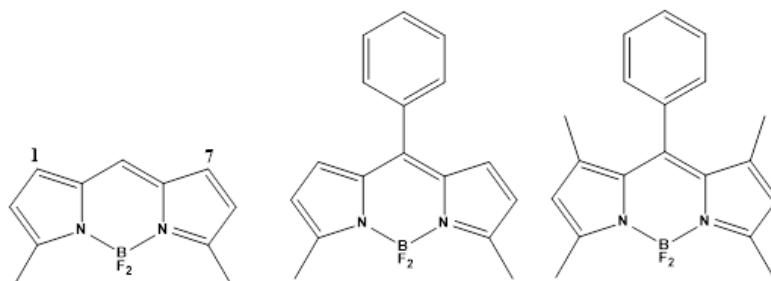
Figure 1.6. Comparison of 1,7 substituted and unsubstituted BODIPY

1.2.2 Electrophilic Substitution on BODIPY

The reactivity of BODIPY depend upo the charge distribution on each of the atoms. The C-2 and C-6 positions of BODIPY reveal that they bear least positive charge in the following resonance structures (Figure 1.7), so these two positions are most favourable for electrophilic attacks.
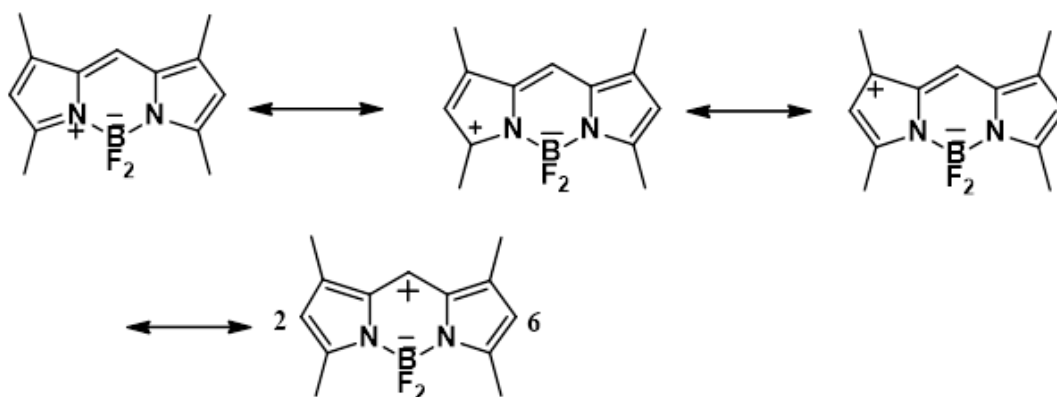
Figure 1.7. Available sites for electrophilic attacks

Halogenation on 2- and 6- positions of BODIPY core causes a bathochromic shift of UV absorption and emission maxima, and it reduces the quantum yield by quenching the fluorescence, due to heavy atom effect and Intersystem crossing leading to Phosphorescence. These molecules thus serve as efficient photosensitizers for photodynamic therapy. Halogenation on these two positions are useful for futher functionalization such as metal catalysed Sonogashira, Suzuki and Stille coupling

reactions. In these reactions mono- and di- products can be preferentially formed by using appropriate equivalents of the reagents.

1.2.3. Styryl BODIPY

Synthetic modification of the BODIPY core in order to get the bathochromic shift for absorption and emission in the Near Infrared (NIR) region (600-900 nm) are following:

- Functionalization of the α-, β-, and meso- sites of the BODIPY core to extend the π-conjugation to create a "push-pull" structure
- Introduction of π-extended pyrrole.
- Replacement of the C-8 position of BODIPY core with nitrogen to create aza-BODIPY[812].
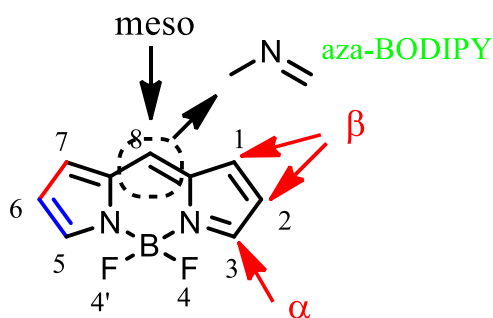
Figure 1.8. General Structure of BODIPY core
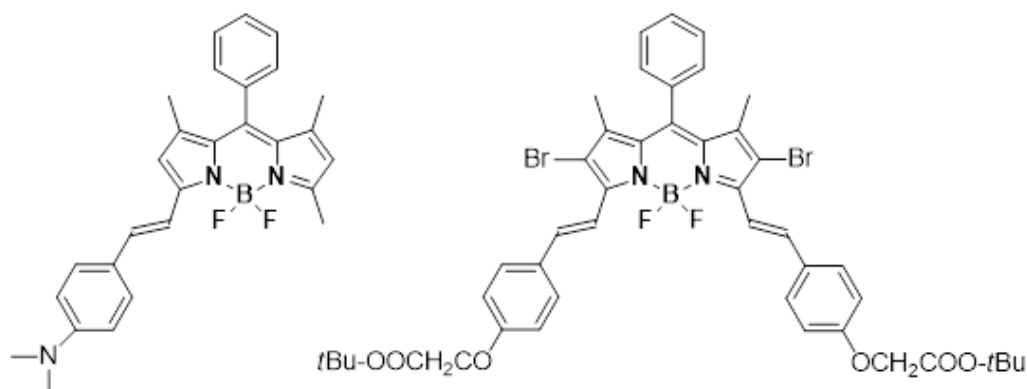
Figure 1.9. Example of π-conjugation extension in BODIPY dyes.

The methyl group on C-3 and C-5 position of BODIPY core are acidic so the Knoevenagel Condensation[11] reactions can be performed in these positions. Piperidinium actetate is used as catalyst in this condensation reaction. The reaction generally gives high yields. Such molecules with extended π-conjugation were

synthesized and owing to their tunable and near infrared absorption and emission properties they can be used as photosensitizers in dye sensitized solar cell (DSSC) and pH sensors.

1.2.3. Application of BODIPY dyes:

BODIPY dyes show excellent properties like high quantum yield, tunable spectral properties. BODIPY dyes are used in fluorescent indicators[13] energy transfer cassettes[14], light emitting diode, photo dynamic therapy[15]. For energy transfer prcocess there are two types, through bond (Dexter type) and through space (Förster type).

Objective of the work:

Polymer solar cells incorporating bulk heterojunction (BHJ) blend based on regioregular poly(3-hexylthiophene) (P3HT) and [6,6]-phenyl-C61-butyric acid methyl ester (PCBM) have been studied widely, and there power conversion efficiency (PCE) using the conventional device fabrication routes are usually in the range of ~ 4-5 %. In 2013, Taylor and co-workers showed for the first time (cite the nature photonics paper) that the efficiency of such polymer solar cells can be enhanced when an additional layer of compound was added in the active layer that could transfer the excitation energy[16]. They made highly efficient polmer solar cells by incorporating a Squaraine (SQ) dye as a energy acceptor and P3HT as a energy donor and after incorporating the SQ, an increase of 38 % was observed in PCE and an efficiency 4.5 % was achieved. Moreover, this system containing a blend of SQ and P3HT as the physically mixed FRET pair was the first such example where FRET was shown to directly influene and increase the PCE of a polymer solar cell. The increased PCE in this FRET based active layer was attributed to improved exciton migration over long distances in such system. Spectroscopic studies revealed that 96% of the excitation energy transfer from P3HT to SQ occurred in this system. After incorporating Squaraine dyes in the active layer of this polymer solar cell, the authors observed increase in PCE and energy transfer efficiency (ETE) because SQ have strong absorbance in the Near Infrared region where P3HT has minimal absorbance therefore, they are complementary absorber pairs and moreover, such complementary absorbers broaden the spectral absorption and thus specyral photoresponse of the solar

cells. In Figure 1.9 (b) the physical mixture i.e., co-solution of P3HT and SQ dye was photoexcited at 525 nm where the SQ absorbs minimally. After successive addition of SQ dye to the P3HT solution, a decrease in the emission intensity of P3HT donor was observed and a concomitant increase in the emission intensity of the SQ acceptor was observed. This observation was indicative of the fact that the P3HT emission was quenching by addition of SQ because of excitation energy transfer from P3HT to SQ. Also, SQ doesn't absorb any light around[1] 525 nm so, the SQ emission intensity increase can be attributed to the resonance energy transfer from P3HT to SQ, which is then the emitted as photons from the SQ. This study was pioneering because or the first time, direct physical mixing of two compounds were shown to enhance the PCE of a polymer or BHJ solar cells.

In this work, the authors chose Squaraine as acceptor because of its promising absorption properties in the NIR region and also it formed a good FRET pair with P3HT cosidering a good spectral overlap between P3HT and squaraine. Because of the promising properties of Squaraine dyes, we have synthesized some Squaraine dyes in our lab and used them as FRET acceptors in our work, as will be explained later. Next, we wanted to design and synthesize FRET donors in such a way so that the donor emission have a good spectral overlap with the acceptor (Squaraine) absorption.

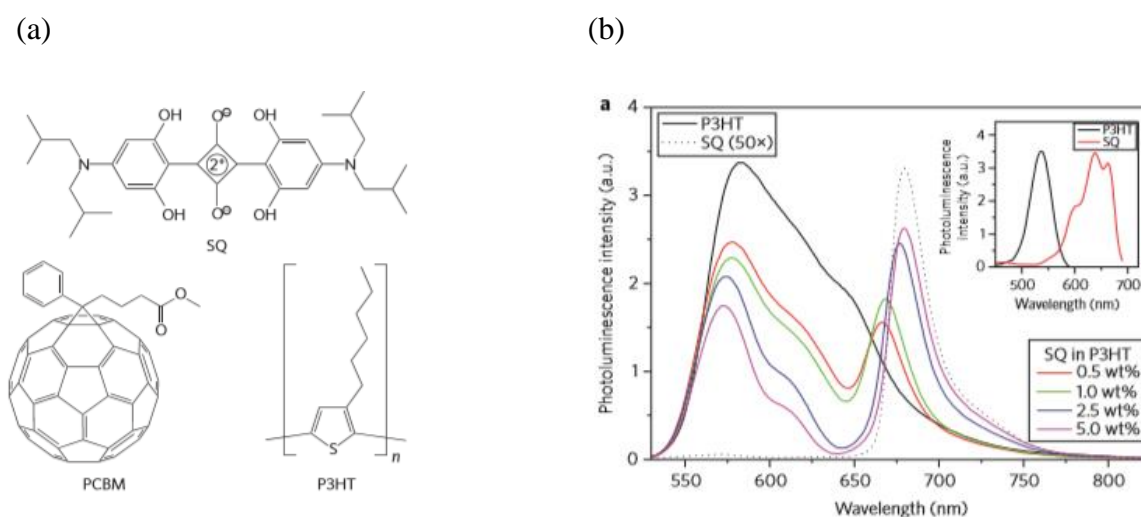(a)   (b)

Figure 1.10. (a) Chemical structure of SQ, PCBM, P3HT. (b) Emission spectra (excite at 525 nm) of pure P3HT (black solid) and pure SQ (black dotted) and P3HT/SQ co-solutions with SQ ratio 0.5-5.0 wt %. (Coutesy: A. Taylor *et al. Nature Photonics* **2013**, *7*, 479-485)

In this work, our focus is to develop new energy donor molecules in order to achieve FRET so that these FRET pairs can be eventually incorporated into the design of bulk heterojunction solar cells. We chose BODIPY dyes as our donor since they show absorption around (300-600 nm). To modify the BODIPY core structure (explained in section 1.2.3) such that their absorption bands can be shifted to near-Infrared region so that they can overlap efficiently with the Squaraine absorption spectra, we adopted the extension of conjugation via the C-3 and C-5 positions of BODIPY. We synthesized a series of the C6-monosubstituted styryl BODIPY compounds as new energy donor molecules. To the best of our knowledge, such C6-monofunctionalized BODIPY with mono-styryl or bis-styryl compounds are not in the literature. An important goal of synthesizing such novel mono substituted styryl-BODIPY (mono-styryl or bis-styryl) is that these are useful synthons to achieve energy transfer dyad or triad cassettes such as DA, DAD and similar kind of molecules. Once the molecules were synthesized, they were purified and structurally characterized. Followed by structural characterization, optical properties were investigated by UV/vis absorption and fluorescence studies. To investigate whether the styrylBODIPY and Squaraine can serve as FRET pairs, we performed fluorescence titration experiments whereby, a solution of acceptor (SQ) was added sequentially in steps of 100 microlitre to a solution of styryl BODIPY and their emission intensities were monitored[16,7]. Eventually, Forster theory was used to calculate the FRET efficiency in all the FRET pairs that were investigated in this work.

Molecular Design in this work:

Two series of styryl BODIPY dyes were synthesized in this work containing mono-and bis styryl groups with solubility inducing hexyl side chains (**3a**-**6a**) and ethylhexyl side chains (**3b**-**6b**). The important feature of all these compounds is that they are mono-functionalized at the C-6 position with either an Iodo substituent (**3a**, **5a**, **3b**, **5b**) or a trimethylsilyl substituent (**4a**, **6a**, **4b**, **6b**) and such monofunctionalized styryl compounds are not known to the best of our knowledge. The difference in side chain (hexyl vs. ethyhexyl) leads to different solubility of these compounds in organic solvents and presumably have very different aggregating properties in thin films and in solid state. Eventually, we characterized these compounds structurally and optically and then

performed FRET studies with three Squaraine dyes (synthesized in our lab) as energy acceptors.
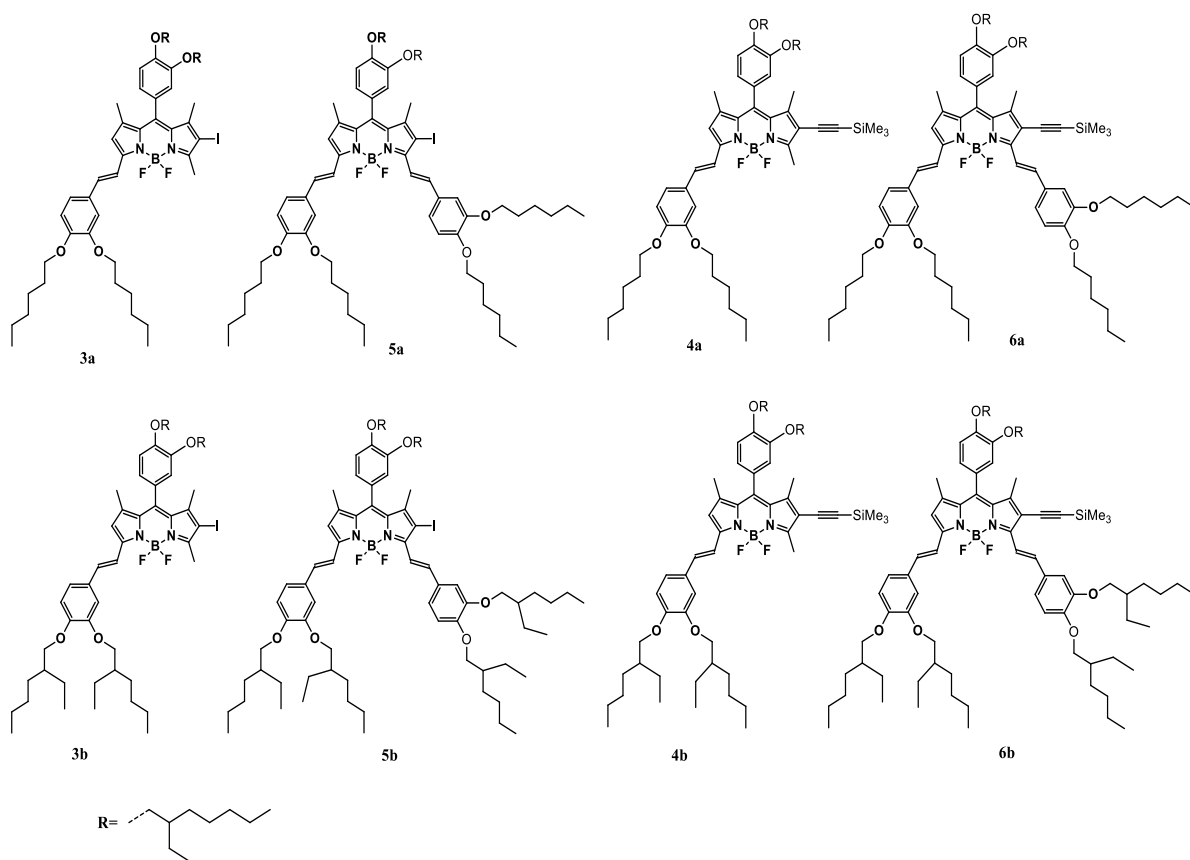
CHAPTER 2

Results and Discussion

StyrylBODIPY dyes have been synthesized inducing hexyl and ethylhexyl chains and monofunctionalization at the C 5-position. NIR styryl BODIPY dyes containing iodo-substituent at C5 position **3a-5a** and **3b-5b** were synthesized by Knoevenagel Condensation reaction, corresponding TMS compounds **4a-6a** and **4b-6b** were synthesized by Sonogashira reaction and all the synthesized compounds were characterized by ^{1}H NMR, ^{13}C NMR, mass spectrometry, UV-vis absorption and fluorescence studies.
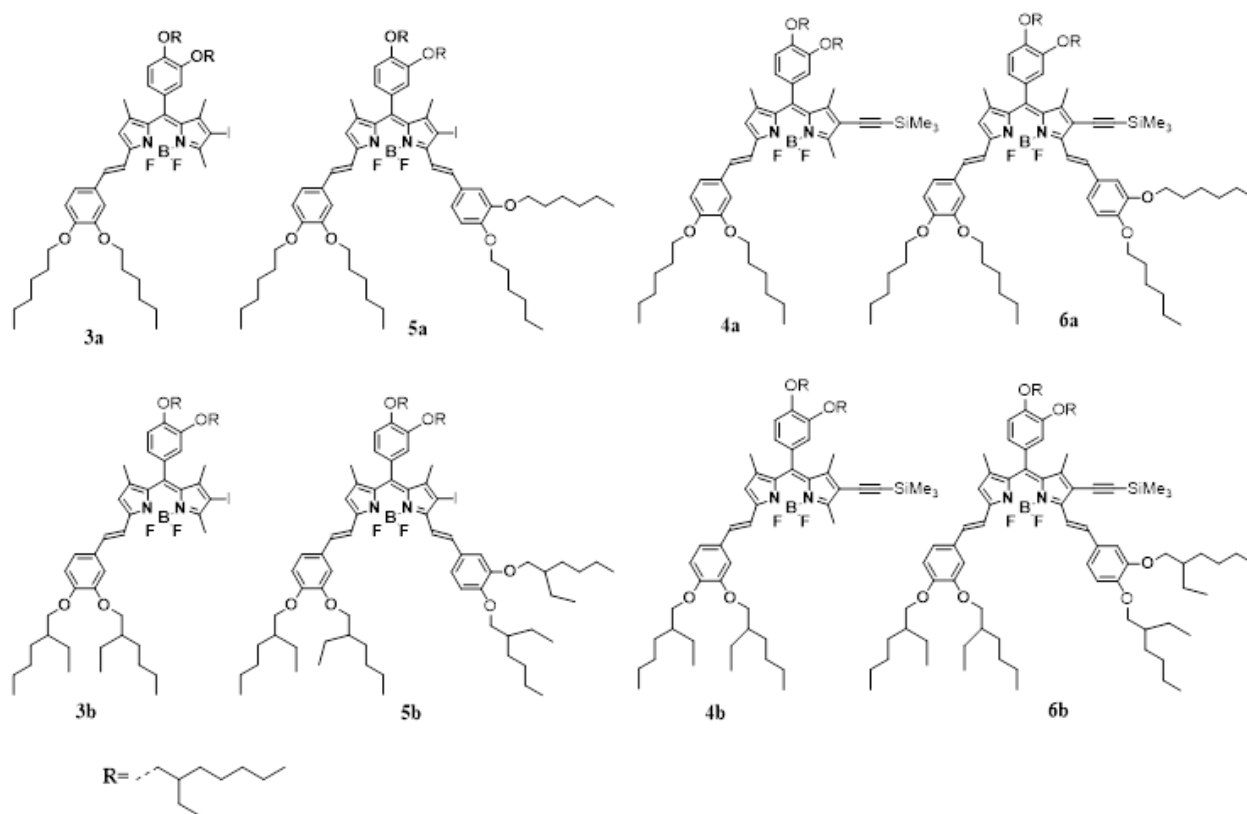
Figure 2.1 All Newly Synthesized chemical structure.

Photophysical Properties of Synthesized compounds :

All synthesized BODIPY compounds were structurally characterized by ^{1}H NMR, ^{13}C NMR, and mass spectrometry and their optical characterization was performed by UV/Vis absorption and fluorescence studies. Squaraine (SQ) dyes as acceptor so that the emission of BODIPY around ~ 650-690 nm overlap significantly with the absorption spectra of SQ that occurs in the range of ~ 660-706 nm. As discussed earlier, good spectral overlap of energy donor emission and energy acceptor absorption is the most important prerequisite of Förster resonance energy transfer (FRET).

The optical properties of all the synthesized styrylBODIPY compounds (mono and di-styryl), as well as their trimethylsilyl-derivatives were investigated by optical spectroscopy. Figure 1 shows the absorption and fluorescence spectra of solution and thin films of compounds **2, 3, 3a, 5a**. Compounds were dissolved in chloroform (c ~ 10^{-5} M) and absorption and emission spectra were recorded. For the emission spectra, compounds **2, 3, 3a, 5a** were excited at 502 nm, 516 nm, 590 nm, 656 nm respectively, where the BODIPY compounds have maximum absorption (λ_{max} absorption).

(a)
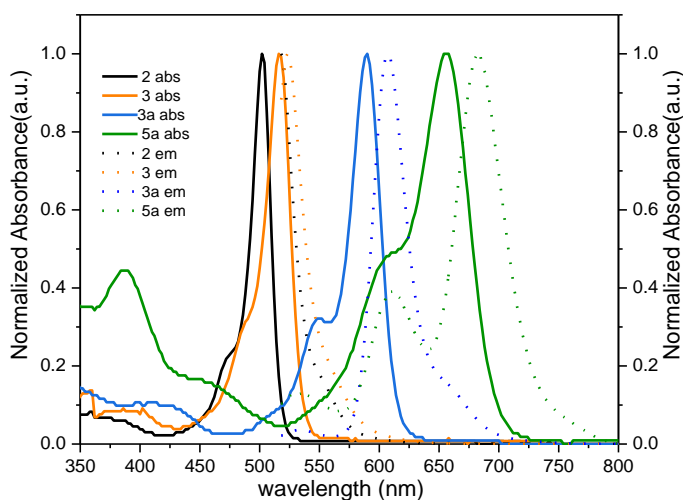
Figure 2.2 Normalized Absorption and Fluorescence spectra of compounds (**2, 3, 3a, 5a**) in CH$_2$Cl$_2$ in 10^{-5} M. Fluorescence spectra of **2,3, 3a, and 5a** were recorded after exciting at 502 nm, 516 nm, 590 nm, 656 nm respectively.
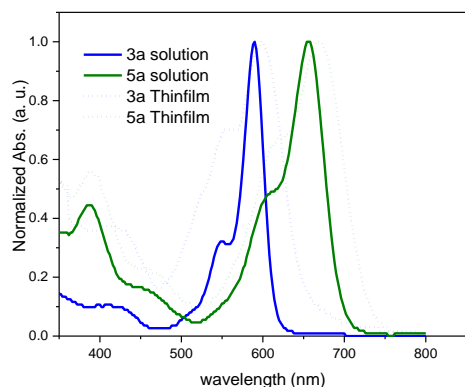
(a)   (b)
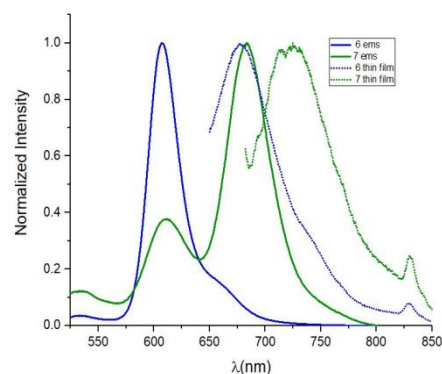
Figure 2.3 (a). Normalized absorption spectra of compounds (**3a, 5a**) in solution (CH_2Cl_2) and thin films. (b). Normalized fluorescence spectra of compounds (**3a, 5a**) in solution (CH_2Cl_2) and thin film. The excitation wavelengths for solutions of compounds **3a, 5a** were 590 nm, 656 nm respectively, and for thin film of compounds were at 608 nm, 682 nm respectively.

Table 2.1 Optical Properties of compounds **2, 3, 3a, 5a**

	Solution			**Thin film**	
Compounds	λ_{abs} (nm)	λ_{em} (nm)	ε ($M^{-1} cm^{-1}$)	λ_{abs} (nm)	λ_{em} (nm)
2	502	512	30800	-	-
3	516	530	96900	-	-
3a	590	607	72400	608	679
5a	656	682	77600	682	721

Absorption and fluorescence data of BODIPY derivatives in solution (CH_2Cl_2) and thinfilm have been compiled in the table 2.1. The Absorption bands of compounds **2, 3** corresponding to S_0-S_1 transition of BODIPY were observed at 506 nm, 516 nm respectively and their emission bands were observed at 512 nm, 530 nm respectively. Comparatively, the absorption bands of compounds **3a**, **5a** showed bathochromically shifted bands at 590 nm and 656 nm respectively, and their corresponding emission

16

bands also showed bathochromic shifts upto 607 nm and 682 nm respectively. The mono-styrylBodipy (**3a**), di-styrylBodipy (**5a**) showed absorption bands in the near infrared (NIR) region due to extention of π–conjugation through the styryl moities. The absorption bands of thin film of compounds **3a**, **5a** showed bathochromic shifts in absorption at 608 nm (vs. 590 nm in solution), 682 nm vs. (656 nm in solution) respectively and emission bands at 679 nm (vs. 607 nm in solution), 721 nm (vs. 682 nm in solution) respectively.

In thin films, compounds usually form aggregates (J- and H- types) and both compounds **3a**, **5a** showed formation of J-aggregates as they showed broad red-shifted emission spectra presented in fig.2.3 (c).

The compounds **3a**, and **6a** are functionalized with hexyl chains in the styryl moieties which can interdigitate efficiently through van der Waals interactions and thus form better π-stacked structures compared to ethylhexyl BODIPY compounds. Thus, due to its better π-stacked structure and tendency to aggregate, their solubilty were decreased in solution compared to ethylhexyl BODIPY compounds. However, owing to the good aggregation in thin films both absorption and emission bands showed significant red shifts in case of hexyl compounds compared to their solution spectra (as discussed above).
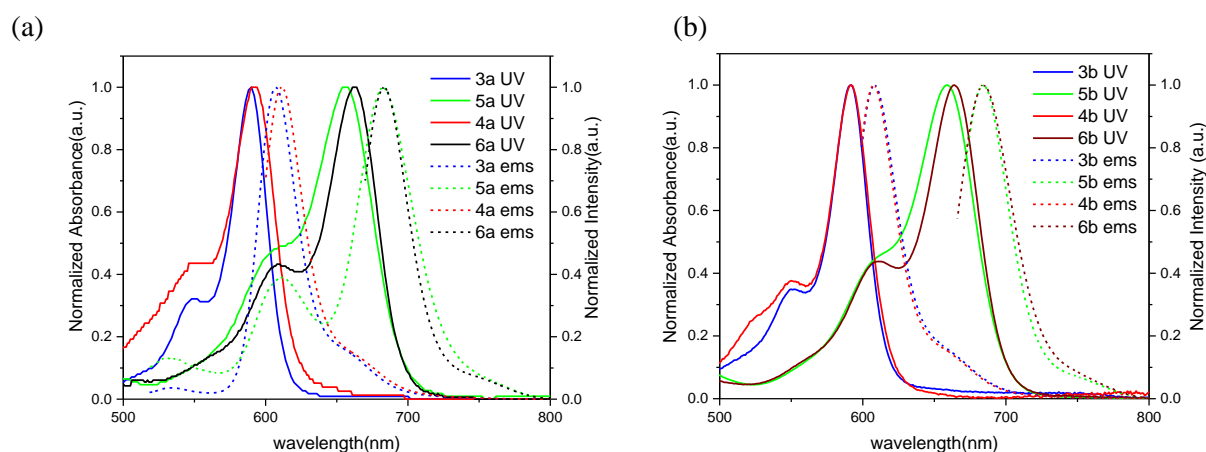
(a) (b)

Figure 2.4 (a)   Normalized absorption and fluorescence spectra of hexyl series BODIPY compounds. (b). Normalized absorption and fluorescence spectra of ethylhexyl series BODIPY compounds.

Table 2.2 Optical properties of mono- and di-styryl BODIPY compounds with hexyl and ethyl hexyl substituents.

Comp-ounds	λ_{abs} (nm)	$\varepsilon(M^{-1}cm^{-1})$	λ_{em} (nm)	Comp-ounds	λ_{abs} (nm)	λ_{em} (nm)	$\varepsilon(M^{-1}cm^{-1})$
2	502	30800	512	**3**	516	530	96900
3a	590	72400	607	**3b**	592	608	42384
4a	592	13019	611	**4b**	593	609	-
5a	656	77600	681	**5b**	659	685	75152
6a	662	32245	683	**6b**	666	686	-

Absorption and emission properties of hexyl series and ethylhexyl series have been compiled in Table 2.2 The Absorption bands of compounds **3a**, **4a** were observed at 590, 592 nm respectively and emission band were observed at 607, 611 nm respectively. The absorption band of compounds **5a**, **6a** were observed at 656 nm, 662 nm respectively and emission bands were observed at 681 nm, 683 nm respectively. The absorption bands of compounds **3b**, **4b** were observed at 592 nm, 593 nm respectively and emission band were observed at 608 nm, 609 nm respectively. The absorption band of compounds **5b**, **6b** were observed at 659 nm, 666 nm respectively and emission band were observed at 685 nm, 686 nm respectively. The compounds (**3a**, **5a**, **3b**, **5b**) have iodo-substituent and thus because of heavy atom effect, the emission was quenched and intensity were much reduced compared to compounds **4a**, **6a**, **4b**, **6b** containing SiMe$_3$ group. The extinction coefficients are calculated by using Beer-Lambert's law:

$$A = \varepsilon*c*l \tag{1}$$

Where, A is the Absorbance, ε is the molar extinction coefficient, c is the concentration of the known solutions, and l is the pathlength. The compounds **2, 3, 3a, 5a** showed molar extinction coefficient values of 30800 cm^{-1}M^{-1}, 96900 cm^{-1}M^{-1}, 72400 cm^{-1}M^{-1} and 77600 cm^{-1}M^{-1}. The data showed that by increasing the π-conjugation the extinction coefficient value also increases. The same trends were also observed for ethylhexyl styryl-BODIPY compounds.

Solvent dependent absorption and emission study of Hexyl-styryl-Bodipy compounds (Solvatochromism):

Solvatochromism is an important property for any class of dye where the permanent dipole moment of the compound in ground state and upon photoexcitation in the excited state are dissimilar. When compounds possess higher dipole moment in the ground state than the excited state, the ground state is preferentially stabilized in polar solvents than non-polar solvents and leads to increase in the optical gaps. As a result, as the solvent polarity is increased, a hypsochromic shift is observed in absorption and emission and this phenomenon termed as negative solvatochromism. However, when the excited state is more polar than the ground state, increasing solvent polarity stabilizes the excited state and leads to lowering of the optical gaps leading to bathochromic shifts in absorption and emission upon going from non-polar to polar solvents. In order to gain insights about the dipole moments of the synthesized molecules, such solvatochromism studies were performed for all compounds of the hexyl styryl bodipy series.

UV-vis absorption of compound **3a** in solvents of different polarities are reported in figure 2.5. Figure 2.5 (a) shows that the in ACN and MeOH, absorption bands were observed at 584 nm, in DCM, THF and toluene solvents the absorption bands were observed at 588 nm, 587 nm, 594 nm respectively. Emission spectra of compound **3a** in different solvents showed that the emission bands observed at 602 nm for both ACN, MeOH, solvents but for DCM, THF, toluene solvents the bands observed at 605 nm, 603 nm, 608. Thus, compound **3a** shows a very weak negative solvatochromism, i.e., by increased solvent polarity a hypsochromic shift in iys absorption and emission bands were observed and this negative solvatochromism can be attributed to a more polar ground state than an excited state. Thus, the ground state is preferentially more stabilized than the excited state in polar solvents leading to increased optical gaps and thus hypsochromic shift as we move from non polar to polar solvents.

Hexyl blue-I

Figure 2.5. Absorption and Emission Spectra of compound **3a**, compound in different solvents acetonitrile (ACN), methanol (MeOH), dichloromethane (DCM), tetrahydrofuran (THF), toluene (Tol). For emission, λ_{exc} was the absorption maxima in a particular solvent

Hexyl blue-TMS

Figure 2.6. Absorption and Emission Spectra of compound **4a**, compound in different solvents acetonitrile (ACN), methanol (MeOH), dichloromethane (DCM), tetrahydrofuran (THF), toluene (Tol). For emission, λ_{exc} was the absorption maxima in a particular solvent.

All other hexyl functionalized styryl bodipy compounds **4a**, **5a**, **6a** also showed similar negative solvatochromism like compound **3a** and the spectra have been compiled in figures 2.6, 2.7 and 2.8 and the spectral shifts for all compounds in different solvents have been compiled in table 5**.**
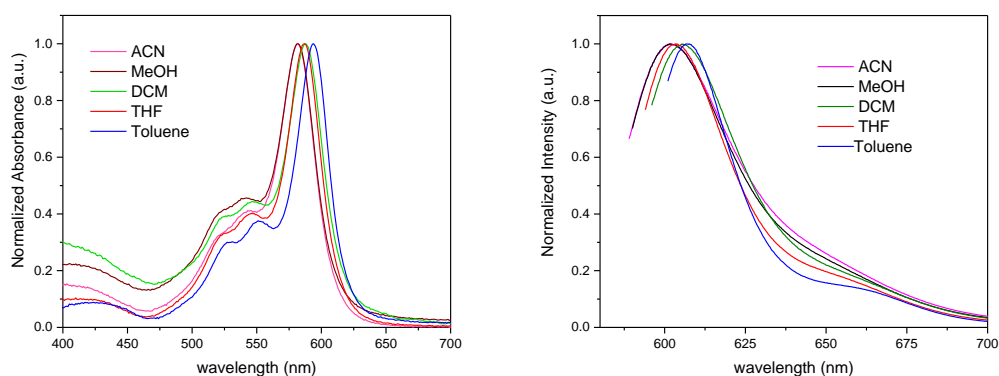
Hexyl green-I

S

Figure 2.7. (a). Absorption and Emission Spectra of compound **5a**, compound in different solvents acetonitrile (ACN), methanol (MeOH), dichloromethane (DCM), tetrahydrofuran (THF), toluene (Tol). For emission, λ_{exc} was the absorption maxima in a particular solvent.
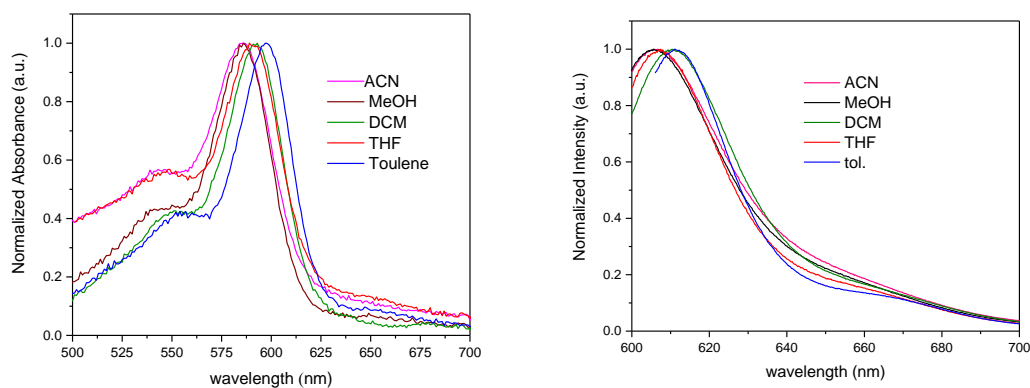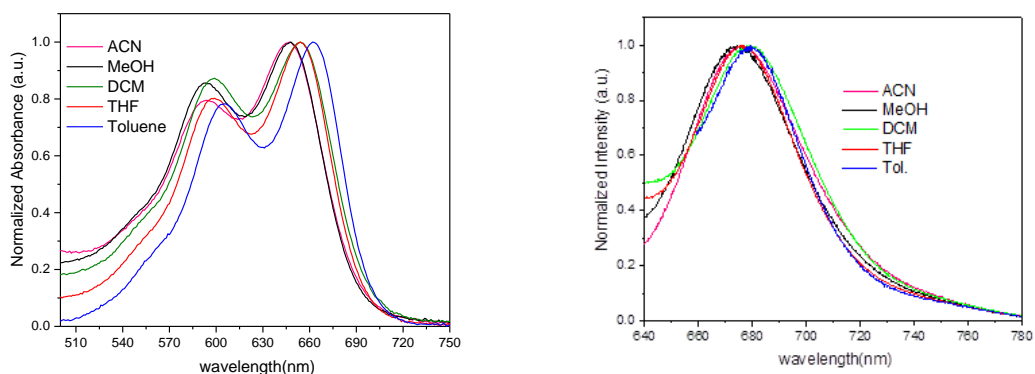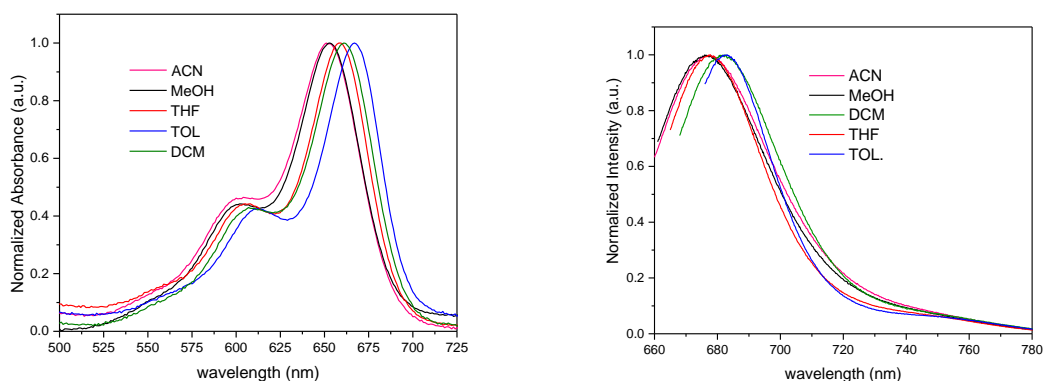
Hexyl green-TMS

Figure 2.8 (a). Absorption and Emission Spectra of compound **6a**, compound in different solvents acetonitrile (ACN), methanol (MeOH), dichloromethane (DCM), tetrahydrofuran (THF), toluene (Tol). For emission, λ_{exc} was the absorption maxima in a particular solvent.

Table 2.3 Solvent dependent study for Hexyl Series compounds.

	Compound 3a		Compound 5a		Compound 4a		Compound 6a	
Solvents	λ_{abs} (nm)	λ_{em} (nm)	λ_{abs} (nm)	λ_{em} (nm)	λ_{abs} (nm)	λ_{em} (nm)	λ_{abs} (nm)	λ_{em} (nm)
ACN	584	602	648	679	590	609	651	680
MeOH	584	602	648	679	588	609	653	680
DCM	588	605	655	682	595	613	661	683
THF	587	603	654	679	595	608	662	680
Toluene	594	608	662	682	602	619	667	684

Development of SQ compounds as energy acceptor compounds:

Previously, three squaraine dyes, have been developed and synthesized in our lab that showed near IR (NIR) absorption and emission and are very well-suited to be studied as energy acceptors with the styryl BODIPY compounds developed in this thesis. Fig 2.9 shows the chemical structures of three squaraine dyes **SQ2**, **SQ4** and **NIRSQ** and Fig 2.10 shows the absorption spectra of these three compounds in chloroform (c ~ 10^{-5} M). SQ2 and SQ4 showed absorption maxima at 650 nm while NIRSQ showed an absorption maximum at 725 nm.

SQ2   **SQ4**
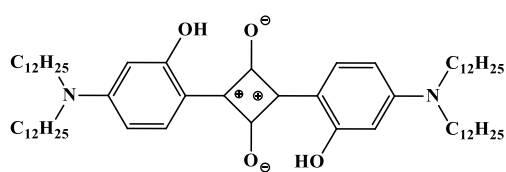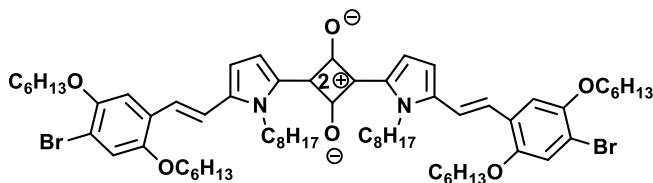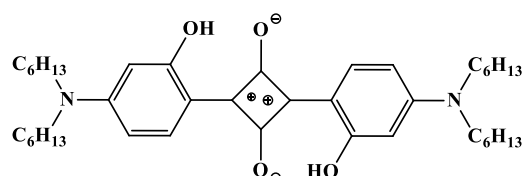
Figure 2.9. Chemical Structures of **SQ2, SQ4, NIRSQ**.

Figure 2.10. Normalized Absorption Spectra of **SQ2, SQ4, NIRSQ**.

Fluorescence Titration of Donor with Acceptor: (Co-solution FRET Study)

According to Förster theory, spectral overlap between energy donor emission and acceptor absorption is directly indicative of the extent of excitation energy transfer that is possible from the donor to the acceptor. Figure 2.11 (a) shows the overlap between emission of compound **4a** and absorption of **SQ2** where the shaded area under the curve is the s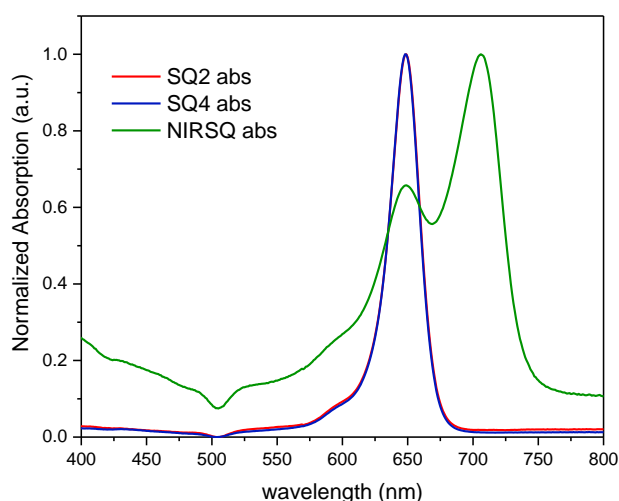pectral overlap. To experimentally verify whether FRET was happening in this case, fluorescence titration of **4a** with addition of **SQ2** was performed. A careful choice of excitation wavelength was necessary for this study such that at a particular excitation wavelength, only the donor is selectively excited and not the acceptor. From the fig 2.10 (UV graph of SQ2, SQ4 and NIRSQ), it is observed that at 425 nm, these SQ compounds have very minimal absorption thus it was chosen as the excitation wavelength for the co-solution FRET studies. With increasing acceptor addition, emission spectra of the co-solution was measured upon excitation at the carefully selected wavelength. Compound **4a** in $CHCl_3$ (c ~ 10^{-5} M) was excited at 425 nm because upon excitation at 425 nm, styryl BODIPY has significant emission whereas **SQ2** has no emission upon excitation at this wavelength. Compound **4a** showed emission band around 590 nm while **SQ2** did not show any detectable emission in the region of 680 nm. To the pure **4a**, **SQ2** in $CHCl_3$ (c ~ 10^{-5} M) was sequentially added in steps of 100 μL and emission spectra of the co-solutions (exciting at 425 nm) were recorded after every addition. A decrease in the

intensity of donor emission band was observed with concomitant increase in the acceptor intensity with increasing content of **SQ2**. However, as already discussed above that 425 nm excitation is not capable of exciting the **SQ2** compound. Thus, the decrease of BODIPY emission intensity and increase of **SQ2** emission intensity can only be attributed to Förster resonance energy transfer from BODIPY **4a** to **SQ2** therefore leading to quenching of the donor fluorescence and increase of the acceptor fluorescence. This behavior is observed by sequential addition of **SQ2** from 100 μL upto 11 mL until the fluorescence of the BODIPY **4a** was almost completely quenched (Fig 2.11 (b)). Using the integrated area under the curve of fluorescence for the pure donor and the co-solution containing donor in presence of acceptor for which the donor emission was almost completely quenched, the FRET efficiency was calculated. FRET efficiency was found to be ~ 68 % for the co-solution of **4a** and **SQ2** and thus **4a** + **SQ2** was a reasonable efficient FRET pair 1.
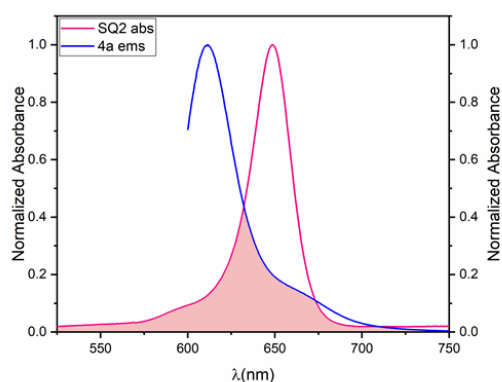
(a)   (b)

Figure 2.11. (a). Spectral overlap of compound **4a** emission and SQ2 absorption. (b). Emission spectra (excite at 425 nm) of compound 4a (21 μM)-only (red), and 4a (21 μM)/SQ2 co-solutions in chloroform.
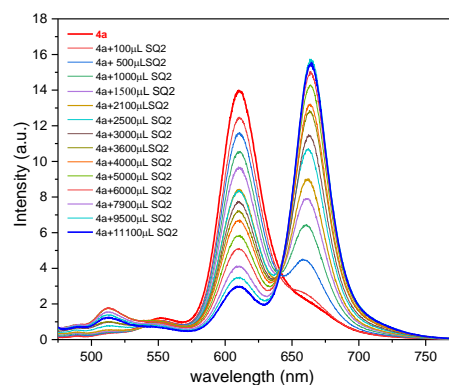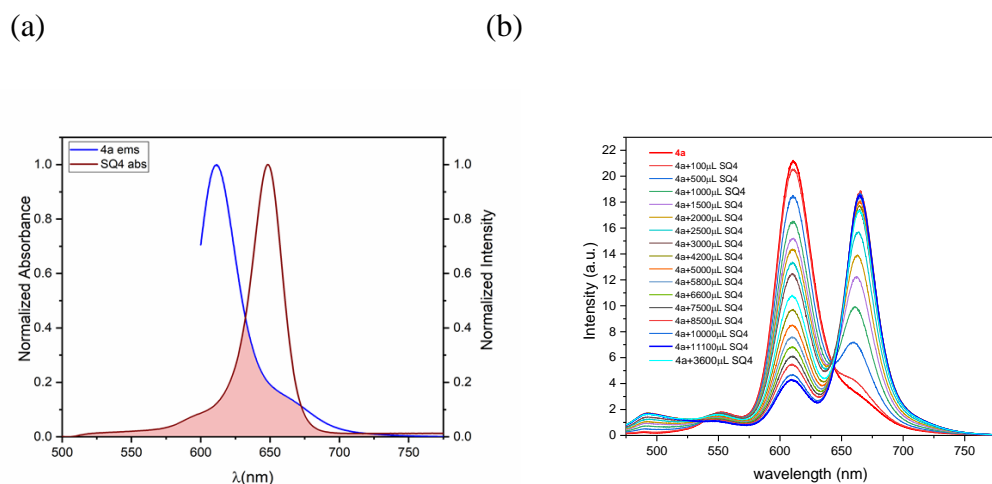
Figure 2.12. (a). Spectral overlap of compound **4a** emission and **SQ4** absorption. (b). Emission spectra (excite at 425 nm) of compound 4a (21 μM)-only (red), and 4a (21 μM)/SQ4 co-solutions in chloroform.

Figure 2.12 (a) shows the overlap between emission of compound **4a** and absorption of **SQ4** where the shaded area under the curve is the spectral overlap. To experimentally verify whether FRET was happening in this case, fluorescence titration of **4a** with addition of **SQ4** was performed. With increasing acceptor addition, emission spectra of the co-solution was measured upon excitation at the carefully selected wavelength. Compound **4a** in CHCl$_3$ (c ~ 10^{-5} M) was excited at 425 nm because upon excitation at 425 nm, styryl BODIPY has significant emission whereas **SQ4** has no emission upon excitation at this wavelength. Compound **4a** showed emission band around 590 nm while **SQ4** did not show any detectable emission in the region of 680 nm. To the pure **4a**, **SQ4** in CHCl$_3$ (c ~ 10^{-5} M) was sequentially added in steps of 100 μL and emission spectra of the co-solutions (exciting at 425 nm) were recorded after every addition. A decrease in the intensity of donor emission band was observed with concomitant increase in the acceptor intensity with increasing content of **SQ4**. However, as already discussed above that 425 nm excitation is not capable of exciting the **SQ4** compound. Thus, the decrease of BODIPY emission intensity and increase of **SQ4** emission intensity can only be attributed to Förster resonance energy transfer from BODIPY **4a** to **SQ4** therefore leading to quenching of the donor fluorescence and increase of the acceptor fluorescence. This behavior is observed by sequential addition of **SQ4** from 100 μL upto 11 mL until the fluorescence of the BODIPY **4a** was almost completely quenched (Fig 2.12 (b)). Using

the integrated area under the curve of fluorescence for the pure donor and the co-solution containing donor in presence of acceptor for which the donor emission was almost completely quenched, the FRET efficiency was calculated. FRET efficiency was found to be ~ 55 % for the co-solution of **4a** and **SQ4** and thus **4a** + **SQ4** was a reasonable efficient FRET pair 2.
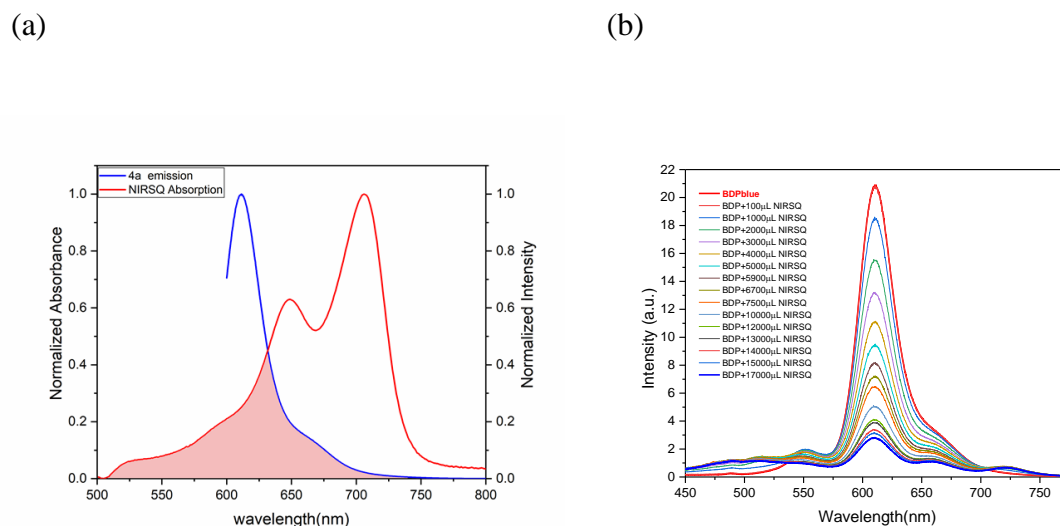
(a) (b)

Figure 2.13.   (a). Spectral overlap of compound **4a** emission and   **NIRSQ** absorption. (b). Emission spectra (excite at 425 nm) of compound 4a (21 μM)-only (red), and 4a (21 μM)/NIRSQ co-solutions in chloroform.

Figure 2.13 (a), shows that the spectral overlap between compound **4a** emission with **NIRSQ** absorption. In figure 2.13 (b), showed experimentally that energy transfer (FRET) is happening in this case. Similar as **4a** + **SQ2** it also excite at 425 nm, showed donor emission around 590 nm and there is no emission detected in the region of 725 nm. So at 425 nm wavelength donor (compound 4a) emission is found but no acceptor (NIRSQ) emission found. So excite the co-solution at 425 nm, observed the decrease in the intensity of donor and increase in the acceptor intensity by increase in every concentration. This behavior is observed over a wide range of NIRSQ concentration varying from 100μL to 11mL. The energy transfer efficiency is found to be 52 % for this *FRET pair 3* (**4a** + **NIRSQ**). It is to be noted that the increment in NIRSQ emission was very little because of the fact that NIRSQ is functionalized with two Br atoms that quench its fluorescence due to significant heavy atom effect and intersystem crossing. Thus, even

though FRET efficiency in case of **4a** + **NIRSQ** was reasonable, eventual emission from NIRSQ was very small.

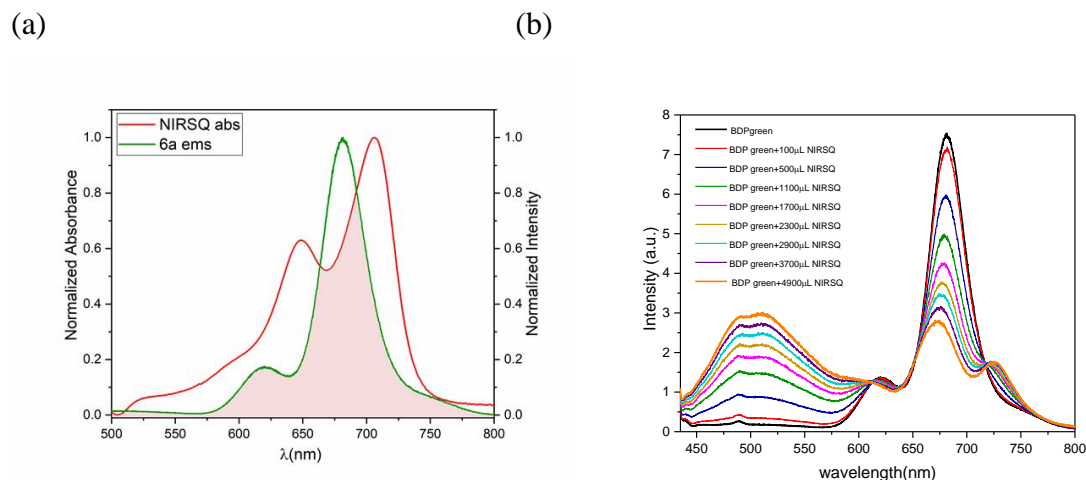(a)   (b)

Figure 2.14 (a). Spectral overlap of compound **6a** emission and **NIRSQ** absorption. (b). Emission spectra (excite at 425 nm) of compound 4a (21 μM)-only (red), and 4a (21 μM)/SQ2 co-solutions in chloroform.

Figure 2.14 (a) shows the overlap between emission of compound **6a** and absorption of **NIRSQ** where the shaded area under the curve is the spectral overlap, it shows the best spectral overlap between donor emission and acceptor absorption in comparison to the spectral overlap of all the other FRET pairs To experimentally verify whether FRET was happening in this case, fluorescence titration of **4a** with addition of **NIRSQ** was performed. A careful choice of excitation wavelength was necessary for this study such that at a particular excitation wavelength, only the donor is selectively excited and not the acceptor. Similar as **4a** + **SQ2** it also excite at 425 nm, showed donor emission around 683 nm and there is no emission detected in the region of 725 nm. So at 425 nm wavelength donor (compound 4a) emission is found but no acceptor (NIRSQ) emission found. This behavior is observed over a wide range of NIRSQ concentration varying from 100μL to 11mL. The energy transfer efficiency is found to be 54 % for this *FRET pair 4*(**6a** + **NIRSQ**). However, NIRSQ contains two bromo substituents thus due to heavy atom effect the compound is inherently very weakly fluorescent and the acceptor emission observed in this case if very weak. Also, the overall FRET efficiency in this case is the lowest among all the compounds (FRET pairs) investigated in this work.

The Energy Transfer Efficiency (ETE) that quantifies the resonance energy transfer from the excited donor to the ground state acceptor via FRET is given by the following equation:

$$ETE = 1 - F_{DA}/F_D \qquad (1)$$

where, F_{DA} is the integrated area under the curve of fluorescence of donor in the presence of acceptor, F_D is the integrated area under the curve of fluorescence of donor in the absence of acceptor. Table x summarizes the FRET efficiencies of all the compounds investigated in this work and the ETE calculated for the **4a + SQ2, 4a + SQ4, 4a + NIRSQ, 6a + NIRSQ** were ~ 68 %, ~ 55 %, ~ 52 % and ~ 54 % respectively thus **4a + SQ2** was the best FRET pair.

Table 2.4. Fluorescence Titration experiment data

FRET pair	Integrated area under fluorescence curve of donor (F_D)	Integrated area under fluorescence curve of donor (F_{DA})	ETE (%) = $1-F_{DA}/F_D$
4a + SQ2	548.85	186.06	68 %
4a + SQ4	516.09	232.24	55 %
4a + NIRSQ	516.09	246.62	52 %
6a + NIRSQ	310.48	138.67	54 %

Chapter 3

Summary and Outlook

In summary, new NIR absorbing and emitting bodipy dyes have been synthesized that are functionalized with styryl moeities containing solubility inducing hexyl and ethylhexyl chains and monofunctionalization at the 5-position. NIR styryl BODIPY dyes containing iodo-substituent at 5 position **3a-xx** and **3b-xx** were synthesized by Knoevenagel Condensation reaction, corresponding TMS compounds xx and xx were synthesized by Sonogashira reaction and all the synthesized compounds were characterized by ^{1}H NMR, ^{13}C NMR, mass spectrometry, UV-vis absorption and fluorescence studies.
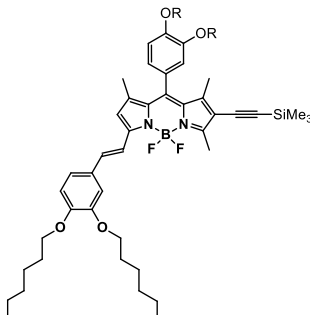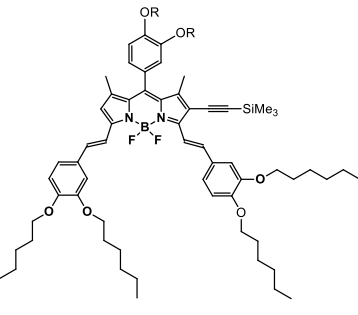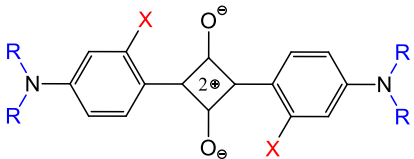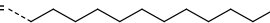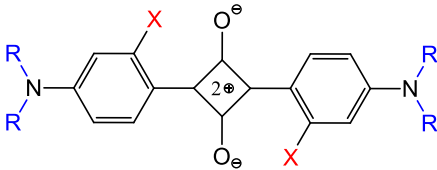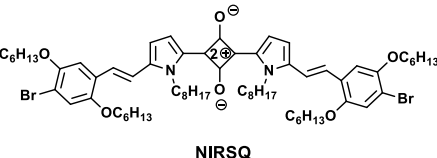
All the compounds showed absorption and emission in the range of ~ 590-690 nm in solution. The NIR styrylBODIPY compounds of ethylhexyl series showed slight bathochromically shifted absorption and emission bands compared to their hexyl counterparts. Furthermore, styryl bodipy iodo compounds xx and xx showed well defined aggregation in thin films. The absorption bands of thin film of compounds **3a**, **5a** showed bathochromic shifts in absorption at 608 nm (vs. 590 nm in solution), 682 nm vs. (656 nm in solution) respectively and emission bands at 679 nm (vs. 607 nm in solution), 721 nm (vs. 682 nm in solution) respectively.

Absorption and fluorescence solvatochromism of compounds **3a, 4a, 5a, 6a** were studied in five solvents of different polarities and all the compounds were observed to show very weak negative solvatochromism. Furthermore, NIR absorbing squaraine dyes **SQ2**, **SQ4** and **NIRSQ** were developed and synthesized that were complementary absorbers to BODIPY dyes and possess narrower optical bandgaps than the bodipy compounds **4a, 6a** thus formed promising energy acceptors. Styryl BODIPY dyes have complementary absorption to SQ dyes, and they show reasonable good spectral overlap with styryl BODIPY emission. Mono-styryl BODIPY and di-styryl BODIPY were designed such that the their emission spectra overlap reasonably with the acceptor Squaraine (SQ) dyes (**SQ2, SQ4, NIRSQ**). Our hypothesis that the newly synthesized monofunctionalized styryl BODIPYs can form efficient FRET pairs with SQ compounds were tested by

performing fluorescence titration experiments. Energy transfer efficiencies for the four FRET pairs were examined by integrated area under the curve analysis of the pure donor emission as well as the emission of donor in the presence of acceptors (i.e., in co-solutions).

Fluorescence Titration of styryl BODIPY **4a, 6a** with Squaraine dyes **SQ2, SQ4, NIRSQ** indicate efficient FRET in co-solutions. Among these four FRET pairs, **4a+SQ2** showed highest ETE of ~ 68 %, other FRET pairs showed ETE of ~ 52-55 %. This study opens the avenues for utilization of such newly designed styryl BODIPY and Squaraine dyes as components of energy transfer in design and synthesis of new FRET cassettes, which we are exploring in our research group now. Interestingly, monofunctionalized BODIPY derivatives are not known to the best of our knowledge and thus they are very useful synthons for the design of small molecular dyads (such as energy donor acceptor), triads (such as ADA) and so on. Finally, owing to their intense emission in the NIR region, such styryl BODIPY compounds have potential applications in bio-labelling and bio- imaging studies which will be explored by us in the future.

Summary of the work

Donor ⟶ Acceptor ↓	BODIPY 4a	BODIPY 6a
SQ2 **SQ2**: X = OH, R =	**4a +SQ2** • Complementary absorption • Good spectral overlap • FRET • ETE = ~ 68 %	• No Bandgap matching • No FRET
SQ4 **SQ4**: X = OH, R =	**4a +SQ4** • Complementary absorption • Good spectral overlap • FRET • ETE = ~ 55 %	• No Bandgap matching • No FRET
NIRSQ **NIRSQ**	**4a +NIRSQ** • Slightly better overlap • FRET • ETE = ~ 52 %	**6a+NIRSQ** • Best spectral overlap • Complementary absorption • FRET • ETE = ~ 54 %

CHAPTER 4

# Experimental Section

General Information:

4.1 Materials

All chemicals and solvents were purchased from commercial suppliers (Sigma Aldrich, SD Fine Chemicals) and used without further purification. Dichloromethane (DCM) was dried over calcium hydride and distilled prior to use. Silica gel of mesh size 60-120 was used for column chromatography. Reactions were monitored in thin layer chromatography (TLC) plates on silica gel and visualized under UV lamp (254 and 365 nm).

4.2 Measurements

The ^{1}H and ^{13}C NMR spectra were recorded on a 400 MHz Bruker Biospin Avance III FT-NMR spectrometer, respectively with TMS as standard at room temperature. The solvent used for NMR was deuterated chloroform ($CDCl_3$). Column chromatography was done with silica gel (60-120) mesh size. Mass spectra was recorded in both ESI positive and negative modes using Waters SYNAPT G2S High Definition HRMS mass spectrometer. UV-Vis was recorded on PerkinElmer LAMBDA 365 UV/Vis spectrophotometer, using a thermostated quartz cuvette with 1 mm path length at 25 ^{0}C. Fluorescence solution measurements were performed with Hitachi F7000 fluorescence spectrophotometer. The spectrometer was equipped with R928F photomultiplier expandable upto 900 nm. Standard software FL Solutions was used for the measurement and analysis of the data. Various excitation wavelengths were used to perform the fluorescence measurements.

4.3   Synthesis
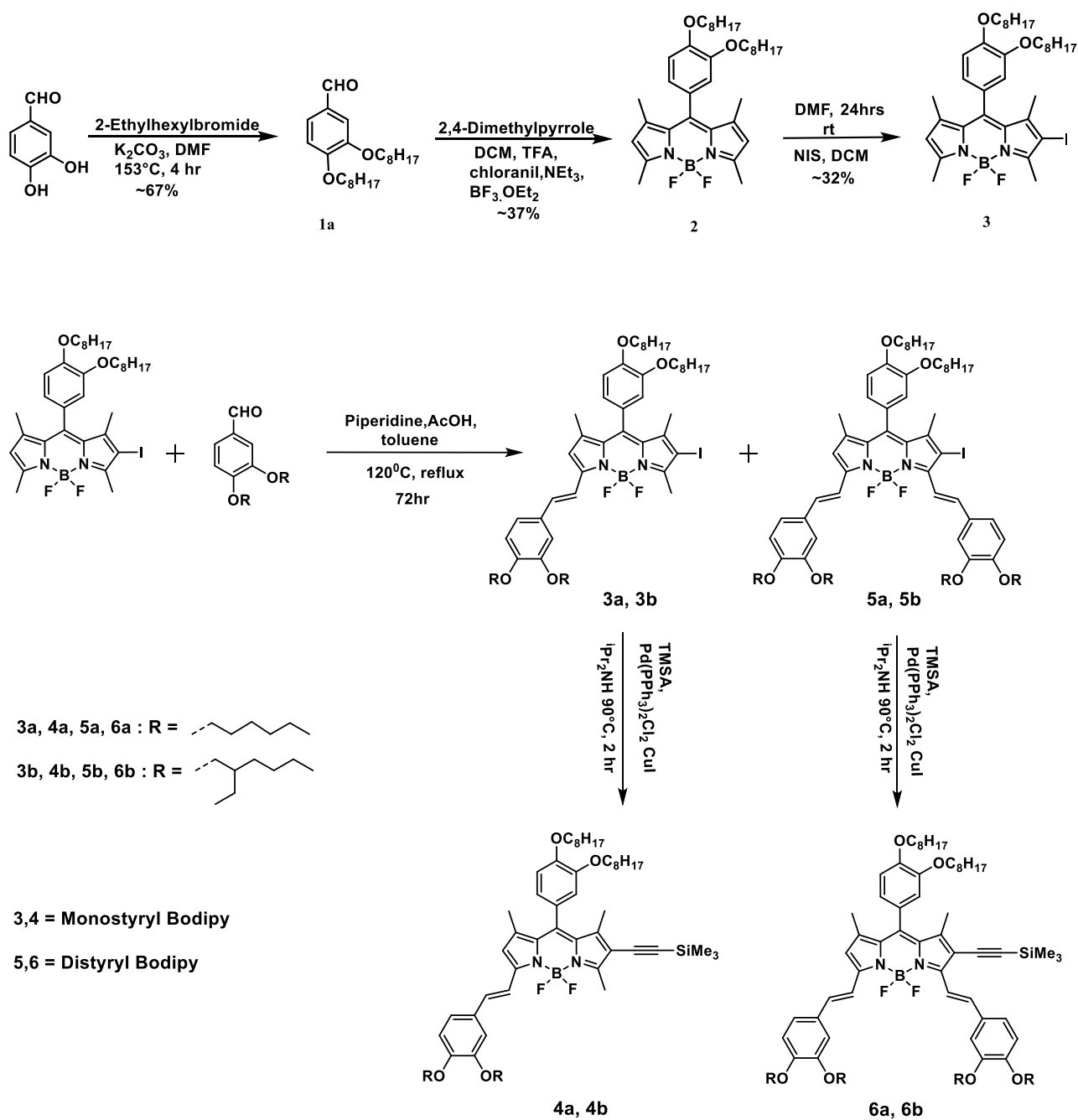
Scheme 4.1.   General reaction scheme for all the compounds synthesized in this work.

Synthesis of BODIPY compound
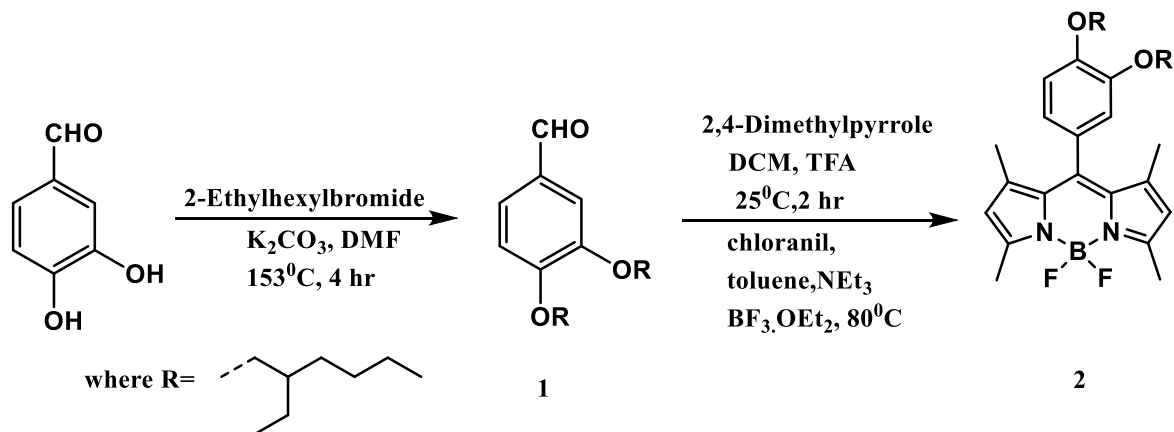
Scheme 4.2. Synthesis of BODIPY (2)

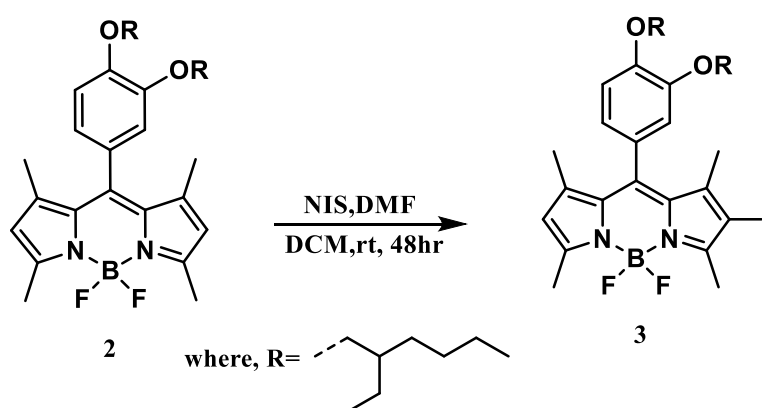**Synthesis procedure of compound 1:**

3,4-dihydroxybenzaldehyde (1.0 g, 7.24 mmol), K_2CO_3 (4.00 g, 28.96 mmol), and 2-ethylhexylbromide (3.35 g, 17.37 mmol) in DMF (15-20 mL) were refluxed at 153 °C, for 4 hours. The reaction mixture was extracted with ethylacetate and ice cold water was added and the aqueous layer was neutralized with saturated sodiumbicarbonate ($NaHCO_3$) solution and organic layer washed with saturated brine solution. The organic layer was dried over sodium sulphate (Na_2SO_4) and solvent was removed at the rotary evaporator. The crude product obtained was subjected to silica gel column chromatography and ethylacetate / hexane 10/90 (v /v) as eluent. The compound **2** was yellow oil obtained with a yield of 62 %.^{1}H NMR (400 MHz, $CDCl_3$): δ (ppm) 9.83 (s, 1 H), 7.40 (s, 2 H), 6.95 (s, 1 H), 3.93 (s, 4 H), 1.78 (s, 2 H), 1.43-1.33 (m, 16 H), 0.92 (s, 12 H).

Synthesis procedure for compound 2:

The compound 1 (1.53 g, 3.89 mmol), 2,4-dimethylpyrrole (0.813 g, 8.55mmol) was dissolved in dry dichloromethane (DCM) (10-15mL) , added 68 μL trifluoroacetic acid (TFA) and stirred at room temperature (RT) for 2 hours. Tetrachloro-1,4-benzoquinone (chloranil) (1.042g, 4.24 mmol) was added to the reaction mixture and stirred for 30 min. Then the DCM was evaporated under reduced pressure. Subsequently, the DPM was

dissolved in 80mL of toluene and triethylamine (1.619 mL) was added. The reaction mixture was stirred for 15 min, followed by addition of, $BF_3.OEt_2$ (2.390 mL) and stirred at 80°C for 30 min. The product formation was monitored by checking the TLC and once the product was formed, water was added in the reaction mixture, heating was stopped and stirred at room temperature for 3 hours. The reaction mixture was extracted with DCM and the aqueous layer was neutralized with saturated $NaHCO_3$ solution and organic layers washed with saturated brine solution. The organic layers were dried over sodium sulphate and solvent was removed at the rotary evaporator. The crude product obtained was subjected to silica gel column chromatography with DCM/ hexane 10/90 (v/v) as eluent to obtain the Bodipy compound **2** in 36 % yield. ^{1}H NMR (400 MHz, CDCl_3): δ (ppm) 6.95 (d, J = 8Hz, 1 H), 6.75-6.73 (m, 2H), 3.92 (d, J = 6Hz, 2 H), 3.80 (m, J = Hz), 2.62 (s, 3 H), 2.55 (s, 3 H), 1.81-1.25 (m, 24 H), 0.96-0.85 (m, 12 H).

Synthesis of BODIPY-I compound 3

Scheme 4.3 Synthesis of BODIPY-I (3)

Synthesis procedure of BODIPY-I:

Compound 2 was dissolved under nitrogen atmosphere in dry DCM and a solution of N-iodosuccinimide (NIS) in dry dimethylformamide (DMF) was added. The solution was stirred for 48 hours at room temperature. The reaction mixture were extracted with DCM, ice cold water was added to remove DMF and the aqueous layer was neutralized with saturated $NaHCO_3$ solution and organic layers washed with saturated brine solution. The organic layer was dried over Na_2SO_4 and solvent was removed at the rotary evaporator. The crude product obtained was subjected to silica gel column chromatography with DCM/ hexane 25/75 (v/v) as eluent to obtain the BODIPY-I compound in 32 % yield. [1]H

NMR (400 MHz, CDCl$_3$): δ (ppm) 6.97 (d, J = 8.8Hz, 1 H), 6.75-6.74 (m, 2 H), 6.04 (s, 1 H), 3.92 (d, J = 8 Hz, 4 H), 3.81 (m, 2 H) 2.63 (s, 3 H), 2.56(s, 3 H), 1.81-1.26 (m, 24 H), 0.98-0.88 (m, 12 H). ^{13}C NMR (400MHz, CDCl$_3$): δ (ppm) 157.65, 154.40, 150.48, 150.34, 145.43, 143.36, 141.97, 132.32, 131.40, 126.86, 122.20, 120.34, 113.94, 113.17, 84.22, 72.18, 71.96, 39.75, 39.66, 30.77, 30.67, 29.34, 29.25, 24.08, 23.99, 23.19, 23.17, 16.89, 15.90, 14.90, 14.86, 14.25, 14.22, 11.40, 11.30.

Knoevenagel Condensation reaction of Hexyl BODIPY compounds :
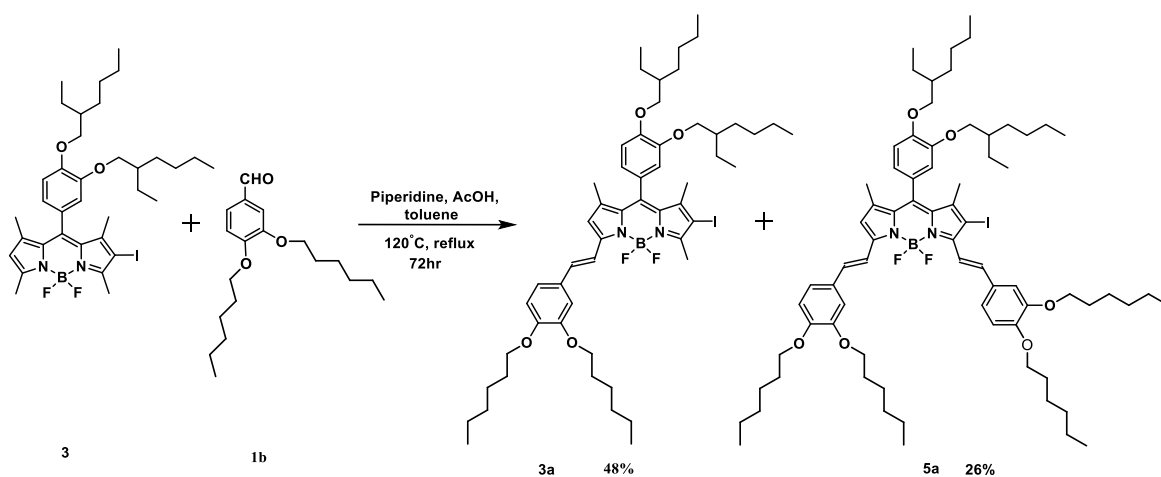
Scheme 4.4 Knoevenagel Condensation reaction of Hexyl BODIPY compounds

Table 4.1: Otimization Table for Knoevenagel Condensation reaction of Hexyl BODIPY compounds

	Comp. 3 Eq.	Comp. 1b Eq.	Acetic acid Eq.	Piperidine Eq.	Reaction Time (hours)	Results
Method 1	1	4	47	27	12	Did not work
Method 2	1	6	24	69	72	Worked
Method 3	1	4	93	134	72	Worked

**Synthesis procedure of BODIPY compound 3a and compound 5a:**

Method 1: Solution of compound 3 (0.05 g, 0.07 mmol) and compound 1b (0.117 g, 0.35 mmol) in dry toluene (10-15mL), acetic acid (0.18 mL, 3.30 mmol) and Piperidine (0.19 mL,1.93 mmol) were added under a N_2 atmosphere. The reaction mixture was refluxed for12 hours at 110^oC and, Dean Stark trap was used to remove the water generated by the condensation. In the beginning, the color of the reaction was orange. After 24 hours, the reaction mixture was red-violet in color. TLC showed one spot after the reaction. The reaction mixture was extracted with DCM and the aqueous layer was neutralized with saturated $NHCO_3$ solution and organic layers washed with saturated brine solution. The organic layer was dried over Na_2SO_4 and solvent was removed at the rotary evaporator. After the workup TLC showed two spots, upper spot was orange in color and lower spot was violet color. The two spots were separated using column chromatography using DCM/Hexane 30/70 (v/v). After checking NMR, starting material was found to be present.

Method 2: Solution of compound 3 (0.05 g, 0.07 mmol) and compound 1b (0.174g, 0.42mmol) in dry toluene (10-15 mL), acetic acid (0.098 mL, 1.724 mmol) and piperidine (0.469 mL, 4.767 mmol) were added under a N_2 atmosphere. The reaction mixture was refluxed for 72 hours at 120^oC, and a Dean Stark trap was used to remove the water generated by the condensation. In the beginning, the color of the reaction was orange. After 24 hours, the reaction mixture turned red-violet in color. After 72 hours, the reaction mixture was blue-green in color. The reaction mixture was extracted with DCM and the aqueous layer was neutralized with saturated $NaHCO_3$ solution and organic layer washed with saturated brine solution. The organic layer was dried over Na_2SO_4 and solvent was removed at the rotary evaporator. After the workup, TLC showed two spots, upper spot was orange color and lower spot was blue in color. The two spots were separated by column chromatography using DCM/hexane 30/70 (v/v). After analysing the NMR, first spot was found to be the starting material, and second spot was found to be mono substituted BODIPY (3a) containing little unreacted benzaldehyde.

Method 3: Solution of compound 3(0.1 g, 0.13 mmol) and compound 1b (0.174 g, 0.52 mmol) in dry toluene (10-15mL), acetic acid (0.694 mL, 12.147 mmol) and piperidine (1.725 mL, 17.47 mmol) and $Mg(ClO_4)_2$ were added under a N_2 atmosphere. The reaction mixture was refluxed for 72 hours at 110^oC, and a Dean Stark trap was used to remove

the water generated by the condensation. In the beginning, the color of the reaction was orange. After 24 hours, the reaction mixture turned red-violet in color. After 72 hours, the reaction mixture was blue in color. The reaction mixture was extracted with DCM and the aqueous layer was neutralized with saturated $NaHCO_3$ solution and organic layers washed with saturated brine solution. The organic layer was dried over Na_2SO_4 and solvent was removed at the rotary evaporator. After the workup TLC showed three spots, upper spot was orange color, the middle one was blue in color and the lower spot was green in color. The three spots were separated using column chromatography using DCM/hexane 30/70 (v/v). The compound 3a was obtained as blue color viscous solid, 46% yield. ^{1}H NMR (400 MHz, $CDCl_3$): δ (ppm) 7.52-7.48 (d, $J = 16$ Hz 1 H), 7.43-7.40 (m, 2 H), 7.20-7.13 (m, 2 H), 6.99-6.42 (m, 2 H), 6.87 (d, $J = 8$ Hz, 1 H), 6.78 (s, 1 H), 6.64 (s, 1 H), 4.10-4.03 (m, 6 H), 3.94 (d, 1 H, $J = 8$ Hz), 3.83 (s, 1 H), 2.67 (s, 3 H), 1.87-1.80 (m, 6 H), 1.51-1.35 (m, 37 H), 0.94-0.88 (m, 18 H). ^{13}C NMR (400 MHz, $CDCl_3$) : δ (ppm) 155.10, 154.69, 153.13, 150.83, 150.24, 150.12, 149.40, 149.23, 144.50, 142.10, 139.72, 138.24, 129.30, 129.82, 129.27, 127.0, 126.68, 122.04, 120.51, 113.71, 113.30, 112.23, 111.26, 110.79, 72.03, 71.81, 69.45, 69.10, 39.61, 31.95, 31.65, 31.60, 31.54, 30.64, 30.54, 29.72, 29.39, 29.29, 29.15, 28.94, 25.75, 25.67, 25.63, 23.95, 23.86, 23.08, 22.72, 22.60, 15.01, 14.15, 14.08, 14.04, 11.28, 11.19. ESI-TOF: $(M+Na)^+$ of molecular fomula $C_{54}H_{78}BF_2IN_2O_4$: Calculated 1017.4965; found 1017.5278 . The compound 5a was obtained as green color viscous solid, 26% yield. ^{1}H NMR (400 MHz, $CDCl_3$): δ (ppm) 8.0-7.95 (d, $J =20$ Hz, 2 H), 7.57-7.51 (m, 2 H), 7.26-7.22 (m, 1 H), 7.19 (d, $J = 12$ Hz, 2 H), 6.97 (d, $J = 8.8$, 2 H), 6.887 (t, $J = 9$ Hz, 2 H), 6.80 (s, 2 H), 6.67 (s, 1 H), 4.11-4.03 (m, 8 H), 3.94 (d, $J = 4$ Hz, 2 H), 3.83 (s, 2 H), 1.88-1.82 (m, 10 H), 1.51-1.35 (m, 46 H), 0.990-0.88 (m, 24 H). ^{13}C NMR (400MHz, $CDCl_3$): δ (ppm) 154.67, 149.43, 139.25, 130.90, 129.85, 128.83, 126.62, 114.06, 111.72, 110.90, 69.10, 65.53, 39.63, 39.55, 33.83, 31.93, 31.55, 31.52, 30.57, 30.31, 29.70, 29.36, 29.32, 29.16, 29.02, 28.94, 25.75, 25.62, 25.66, 23.06, 22.58, 19.19, 14.12, 14.00, 13.73, 11.27, 11.18. ESI-TOF: $(M+Na)^+$ of molecular fomula $C_{73}H_{106}BF_2IN_2O_6$ Calculated 1305.7054; found 1305.7355.
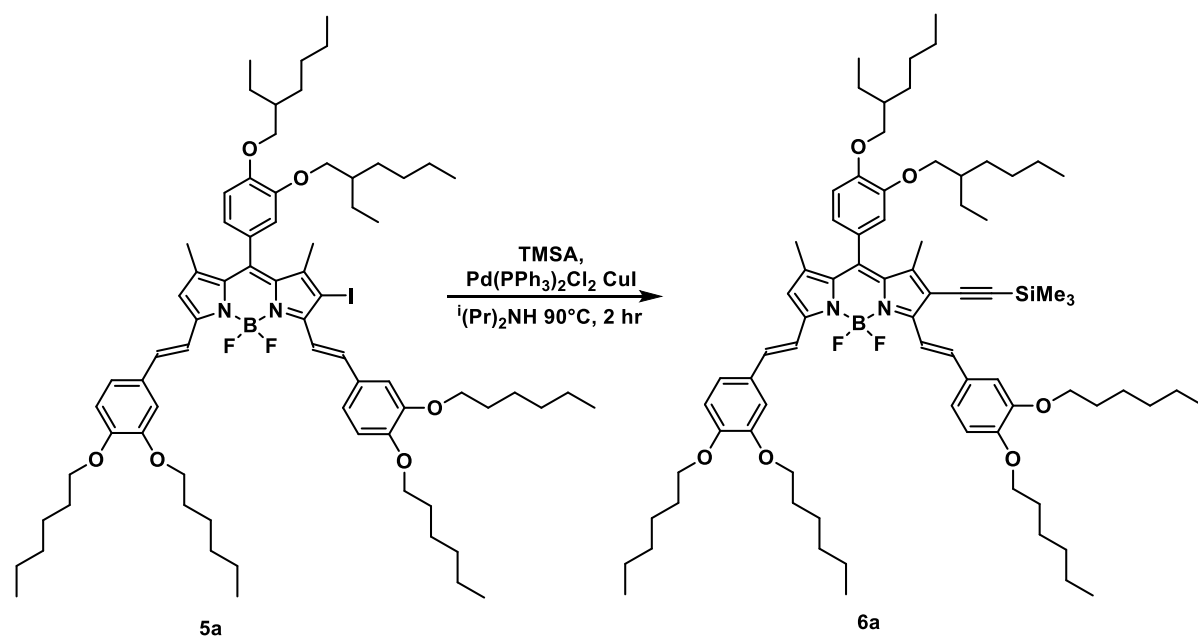
Synthesis of compound (4a):
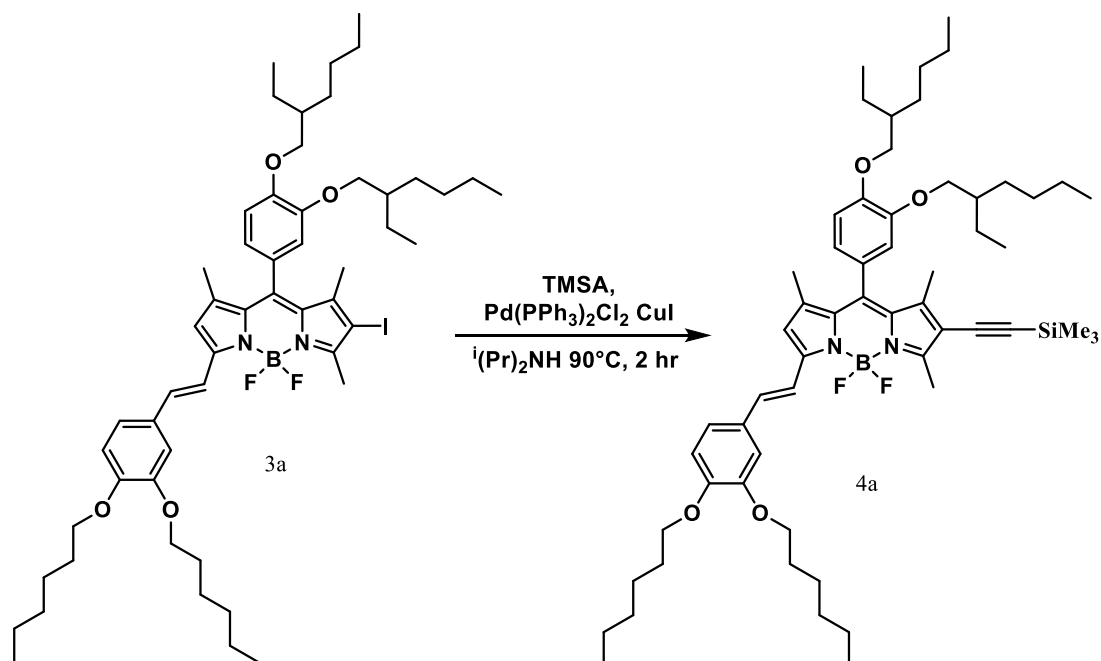
Scheme 4.5 Synthesis of hexyl mono-styrylBODIPY-TMS (4a)

Synthesis of compound 4a:

A solution of compound 3a (0.04 mg, 0.04 mmol), Pd(Ph$_3$P)$_2$Cl$_2$ (1.41 mg, 0.002 mmol) and CuI (0.38 mg, 0.002 mmol) in dry diisopropylamine (50 ml) was stirred under a nitrogen atmosphere and trimethylsilylacetylene (TMSA) (11.42 µl, 0.0802 mmol) was added. The mixture was stirred at 90 °C for 2 h. The solvent was removed under reduced pressure and the crude product was purified by flash-column chromatography PE/CH$_2$Cl$_2$ 80/20 (v/v). The compound 4a was obtained as blue color viscous solid in, ~75 % yield. ^{1}H NMR (400 MHz, CDCl$_3$): δ (ppm) 7.7 (s, 1 H), 7.52-7.48 (d, J = 16 Hz, 2 H), 7.13 (s, 1 H), 6.99 (d, J = 12 Hz, 2 H), 6.8-6.78 (m, 2 H), 6.64 (s, 1 H), 4.04-3.08 (m, 8 H), 2.26 (s, 3 H), 1.83-1.60 (m, 6 H), 1.51-1.31 (m, 37 H), 0.92-0.88 (m, 18 H), 0.22 (s, 6 H). ^{13}C NMR (400 MHz, CDCl$_3$): δ (ppm) 154.47, 149.22, 139.14, 135.66, 129.67, 126.50, 124.61, 124.58, 113.89, 111.47, 110.60, 68.91, 36.92, 34.11, 32.57, 31.76, 31.34, 30.12, 29.87, 29.20, 28.83, 28.75, 26.92, 25.47, 25.44, 22.53, 22.41, 13.96, 13.83. ESI-TOF: (M+Na)$^+$ of molecular fomula C$_{59}$H$_{87}$BF$_2$IN$_2$O$_4$Si Calculated 987.6394 ; Found 987.6584.

Synthesis of compound 6a:

Scheme 4.6 Synthesis of hexyl di-styrylBODIPY-TMS (6a)

Synthesis Procedure of compound 6a: A solution of compound 5a (26 mg, 0.02 mmol), Pd(Ph$_3$P)$_2$Cl$_2$ (0.7 mg, 0.001 mmol) and CuI (0.19 mg, 0.001 mmol) in dry diisopropylamine (40 ml) was stirred under a nitrogen atmosphere and TMSA(5.76μl, 0.04 mmol) was added. The mixture was stirred at 90 °C for 2 h. The solvent was removed under reduced pressure and the crude product was purified by flash-column chromatography using PE/CH$_2$Cl$_2$ 60/40 (v/v). The compound 6a was obtained as green colour viscous solid in ~80 % yield. ^{1}H NMR (400 MHz, CDCl$_3$): δ (ppm) 8.34 (d, J = 16 Hz, 2 H), 7.64-7.54 (m, 2 H), 7.21 (s, 1 H), 7.13 (d, J = 8 Hz, 1 H), 7.00-6.96 (m, 2 H), 6.91-6.87 (t, J= 8 Hz, 2 H), 6.80 (s, 2 H), 6.65 (s, 1 H), 4.08-3.92 (m, 12 H), 1.86-1.83 (m, 10 H), 1.56-1.36 (m, 46 H), 0.93-0.88 (m, 24 H), 0.27 (s, 9 H). ^{13}C NMR (400 MHz, CDCl$_3$): δ (ppm) 150.82, 150.14, 149.18, 135.84, 131.87, 130.46, 129.49, 124.80, 120.62, 114.01, 72.01, 71.97, 71.83, 69.38, 69.11, 39.61, 39.53, 37.79, 37.11, 36.58, 34.31, 33.89, 33.20, 32.76, 31.95, 31.66, 31.63, 31.04, 30.65, 30.57, 30.31, 30.21, 30.19, 30.07, 29.54, 29.40, 29.31, 29.19, 29.13, 28.97, 28.93, 28.66, 27.11, 26.70, 26.57, 25.72, 23.95, 23.92, 22.72, 19.80, 14.16, 13.05, 11.29, 11.20, 10.74, 1.04.

Knoevenagel Condensation reaction of Ethylhexyl BODIPY Compounds

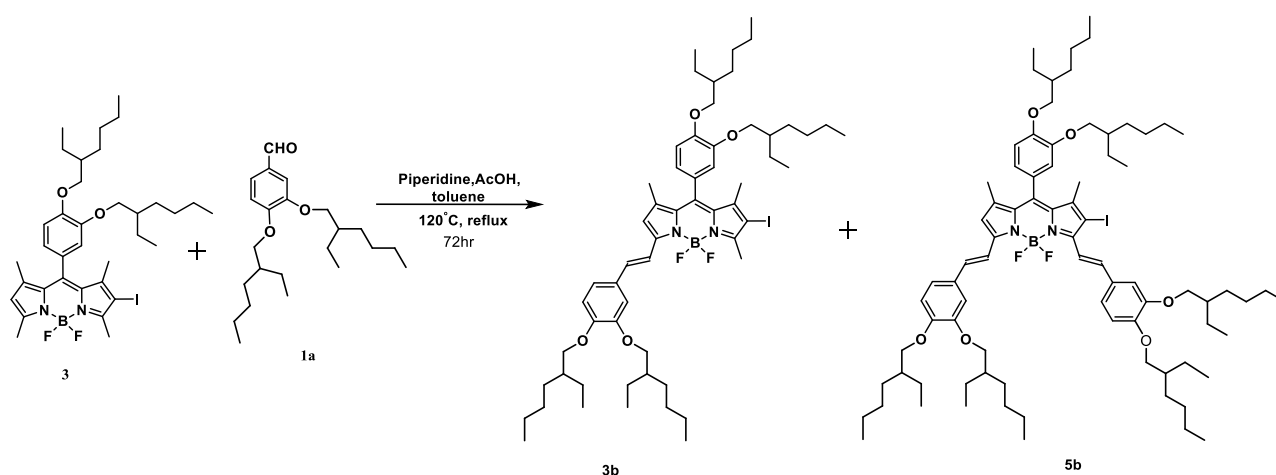**Scheme 4.7 Knoevenagel Condensation reaction of Ethylhexyl BODIPY compounds**

**Table 4.2 Optimization Table for Ethylhexyl Bodipy Knoevenagel condensation reaction**

	Compound 3 (eq.)	Compound 1a (eq.)	Compound 3b (mg)	Compound 5b (mg)
Method 1	1	4	15 (~65%)	19 (~30 %)
Method 2	1	6	22 (~40%)	54 (~60%)

Synthesis Procedure of compound 3b and compound 5b:

Solution of compound 3 (0.1 g, 0.141 mmol) and compound 1a (0.331 g, 0.846 mmol) in dry toluene (30-40 mL), acetic acid (0.753 mL, 13.175 mmol) and piperidine (1.8747 mL,18.9786 mmol) and small amount of anhydrous $Mg(ClO_4)_2$ were added under a N_2 atmosphere. The reaction mixture was refluxed for 72 hours at $120^{\circ}C$, and a Dean Stark trap was used to remove the water generated by the condensation. In the beginning, the colour of the reaction was orange. After 24 hours, the reaction mixture was dark red in colour. After 72 hours, the reaction mixture was blue-green in colour. The reaction

mixture was extracted with DCM and the aqueous layer was neutralized with saturated $NaHCO_3$ solution and organic layers washed with saturated brine solution. The organic layer was dried over Na_2SO_4 and solvent was removed at the rotary evaporator. After the workup TLC showed three spots, upper spot was orange color (starting material), the middle spot was bluein color (fluorescent pink in solution) and the lower spot was dark green in color. The three spots were separated by column chromatography using PE/DCM 75/25 (v/v). The compound 3b was obtained as dark blue viscous solid 22 mg (68%) yield. ESI-TOF: $(M+Na)^+$ of molecular fomula $C_{58}H_{86}BF_2IN_2O_4$ Calculated; 1073.5591 and Found; 1073.5641. The compound 5b was obtained as a dark green viscous 66 mg (60%) yield. ^1H NMR (400 MHz, $CDCl_3$): δ (ppm) 8.01 (d, J = 16 Hz, 2 H), 7.99-7.53 (m, 2 H), 7.20 (s, 1 H), 7.12 (d, J = 12 Hz, 2 H), 6.99-6.17 (d, J = 8 Hz, 2 H), 6.90-6.86 (t, J = 8 Hz, 2 H), 6.81 (s, 2 H), 6.68 (s, 1 H), 3.97-3.84 (m, 12 H), 1.80-1.77 (m, 10 H), 1.52-1.33 (m, 50 H), 0.95-0.91 (m, 36 H). ^{13}C NMR (400MHz, $CDCl_3$): δ (ppm) 155.09, 151.06, 150.41, 150.48, 149.99, 149.38, 143.99, 142.75, 138.43, 136.16, 138.10, 137.43, 134.22, 132.40, 129.99, 129.09, 127.09, 121.31, 120.67, 120.44, 118.61, 117, 116.61, 113.56, 113.20, 112.85, 112.85, 112.64, 71.90, 71.67, 71.55, 71.44, 71.29, 64.31, 39.49, 39.36, 30.52, 30.44, 29.60,29.10, 29.03, 29.0, 25.24, 23.82, 23.75, 22.99, 22.97, 17.05, 14.94, 14.01, 11.17, 11.07. ESI-TOF: $(M+Na)^+$ of molecular fomula $C_{81}H_{122}BF_2IN_2O_6$ Calculated; 1417.8306 Found; 1417.8351.

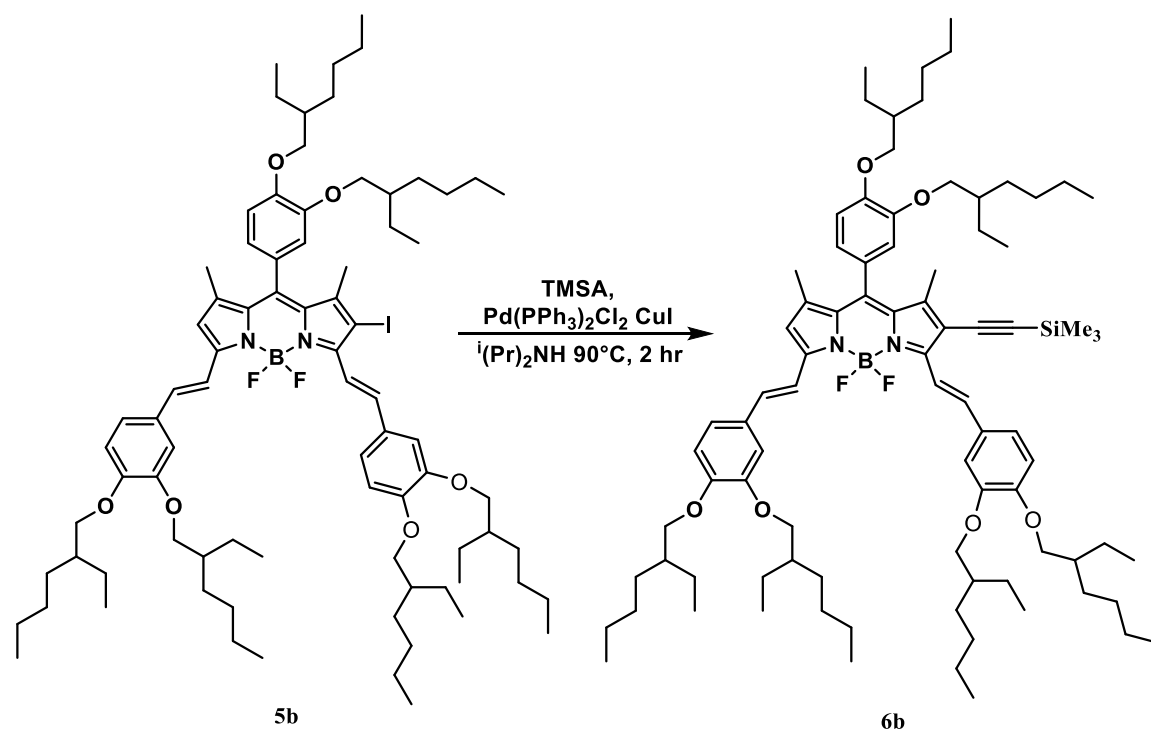**Synthesis of compound 4b:**
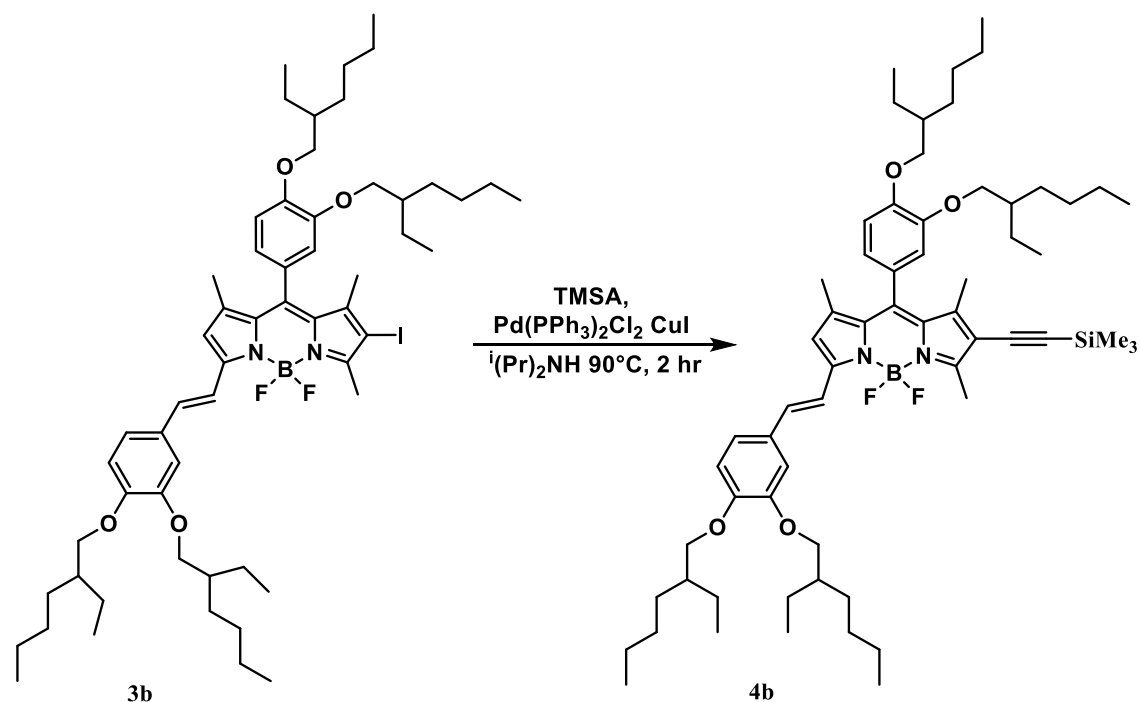
Scheme 4.8 Sythesis of Ethylhexyl mono-styrylBODIPY-TMS (4b)

Synthesis Procedure of compound 4b:

A solution of compound 3b (21 mg, 0.019 mmol), $Pd(Ph_3P)_2Cl_2$ (0.66 mg, 0.00095 mmol) and CuI (0.18 mg, 0.00095 mmol) in dry diisopropylamine (30 ml) was stirred under a nitrogen atmosphere and TMSA(5.4 μL, 0.0381 mmol) was added. The mixture was stirred at 90 °C for 5 h. The solvent was removed under reduced pressure and the crude product was purified by flash-column chromatography PE/CH_2Cl_2 2:1(v/v). The compound 4b was obtained as dark blue viscous solid 5 mg (75%) yield.

Note: Since the amount of pure compound was too little after successive column chromatography purifications, peaks in ^{1}H NMR spectra recorded were too weak to be visible. This compound needs to be scale up to record a good NMR data.

Synthesis of compound 6b:

Scheme 4.8 Sythesis of Ethylhexyl di-styrylBODIPY-TMS (6b)

Synthesis Procedure of compound 6b:

A solution of compound 5b (54 mg, 0.038 mmol), Pd(Ph$_3$P)$_2$Cl$_2$ (1.33 mg, 0.0019 mmol) and CuI (0.36 mg, 0.0019 mmol) in dry diisopropylamine (40 mL) was stirred under a nitrogen atmosphere and TMSA (10.84 µL, 0.0762 mmol) was added. The mixture was stirred at 90 °C for 6 hours. The solvent was removed under reduced pressure and the crude product was purified by flash-column chromatography using PE/CH$_2$Cl$_2$ 60/40 (v/v). The compound 6b was obtained as green colour viscous solid 17 mg (~85 % yield). ESI-TOF: (M+Na+H)$^+$ of molecular fomula C$_{86}$H$_{131}$BF$_2$N$_2$O$_6$Si Calculated; 1388.9813 Found; 1388.9547. ^{1}H NMR (400 MHz, CDCl$_3$): δ (ppm) 8.35 (d, J = 16 Hz, 2H), 7.66-7.52 (m, 3 H), 7.23 (s, 1H), 7.09 (d, J = 16 Hz), 6.98 (s, 1H), 6.90-6.86 (t, J = 8 Hz, 2 H),

6.80 (s, 1 H), 6.65 (s, 1 H), 3.96-3.91 (m, 10 H), 3.83 (s, 2 H), 1.82-1.79 (m, 6 H), 1.51-1.48 (m, 16 H), 1.43-1.33 (m, 36 H), 0.27 (s, 9 H)

References

(1)   Shrestha, D.; Jenei, A.; Nagy, P.; Vereb, G.; Szöllősi, J. *Understanding FRET as a Research Tool for Cellular Studies*; 2015; Vol. 16.

(2)   Perrin, F. 8 Excitation Energy Transfer. **1927**, 1–20.

(3)   Warnan, J.; Buchet, F.; Pellegrin, Y.; Blart, E.; Odobel, F. Panchromatic Trichromophoric Sensitizer for Dye-Sensitized Solar Cells Using Antenna Effect. *Org. Lett.* **2011**, *13* (15), 3944–3947.

(4)   Driscoll, K.; Fang, J.; Humphry-Baker, N.; Torres, T.; Huck, W. T. S.; Snaith, H. J.; Friend, R. H. Enhanced Photoresponse in Solid-State Excitonic Solar Cells via Resonant Energy Transfer and Cascaded Charge Transfer from a Secondary Absorber. *Nano Lett.* **2010**, *10* (12), 4981–4988.

(5)   Isik, M.; Ozdemir, T.; Turan, I. S.; Kolemen, S.; Akkaya, E. U. Chromogenic and Fluorogenic Sensing of Biological Thiols in Aqueous Solutions Using BODIPY-Based Reagents. *Org. Lett.* **2013**, *15* (1), 216–219.

(6)   Li, X.; Traganos, F.; Melamed, M. R.; Darzynkiewicz, Z. Single-step Procedure for Labeling DNA Strand Breaks with Fluorescein- or Bodipy-conjugated Deoxynucleotides: Detection of Apoptosis and Bromodeoxyuridine Incorporation. *Cytometry* **1995**, *20* (2), 172–180.

(7)   Walker, B. J.; Bulović, V.; Bawendi, M. G. Quantum Dot/J-Aggregate Blended Films for Light Harvesting and Energy Transfer. *Nano Lett.* **2010**, *10* (10), 3995–3999.

(8)   Parisotto, S.; Lace, B.; Artuso, E.; Lombardi, C.; Deagostino, A.; Scudu, R.; Garino, C.; Medana, C.; Prandi, C. Heck Functionalization of an Asymmetric Aza-BODIPY Core: Synthesis of Far-Red Infrared Probes for Bioimaging Applications. *Org. Biomol. Chem.* **2017**, *15* (4), 884–893.

(9)   Loudet, A.; Burgess, K. BODIPY Dyes and Their Derivatives: Syntheses and Spectroscopic Properties. *Chem. Rev.* **2007**, *107* (11), 4891–4932.

(10)   Loudet, ‡ Academia Sinica ; Burgess, A.; Ulrich, K.; Ziessel, G.; Harriman, R.

438-441. *Angew. Chem., Int. Ed* **2007**, *107* (1), 39.

(11) Galangau, O.; Dumas-Verdes, C.; Méallet-Renault, R.; Clavier, G. Rational Design of Visible and NIR Distyryl-BODIPY Dyes from a Novel Fluorinated Platform. *Org. Biomol. Chem.* **2010**, *8* (20), 4546–4553.

(12) Shi, W. J.; Lo, P. C.; Singh, A.; Ledoux-Rak, I.; Ng, D. K. P. Synthesis and Second-Order Nonlinear Optical Properties of Push-Pull BODIPY Derivatives. *Tetrahedron* **2012**, *68* (42), 8712–8718.

(13) Boens, N.; Leen, V.; Dehaen, W. Fluorescent Indicators Based on BODIPY. *Chem. Soc. Rev.* **2012**, *41* (3), 1130–1172.

(14) Bessette, A.; Hanan, G. S. Design, Synthesis and Photophysical Studies of Dipyrromethene-Based Materials: Insights into Their Applications in Organic Photovoltaic Devices. *Chem. Soc. Rev.* **2014**, *43* (10), 3342–3405.

(15) Awuah, S. G.; You, Y. Boron Dipyrromethene (BODIPY)-Based Photosensitizers for Photodynamic Therapy. *RSC Adv.* **2012**, *2* (30), 11169–11183.

(16) Huang, J. S.; Goh, T.; Li, X.; Sfeir, M. Y.; Bielinski, E. A.; Tomasulo, S.; Lee, M. L.; Hazari, N.; Taylor, A. D. Polymer Bulk Heterojunction Solar Cells Employing Förster Resonance Energy Transfer. *Nat. Photonics* **2013**, *7* (6), 479–485.

(17) Liu, J.; Tang, B.; Liang, Q.; Han, Y.; Xie, Z.; Liu, J. Dual Förster Resonance Energy Transfer and Morphology Control to Boost the Power Conversion Efficiency of All-Polymer OPVs. *RSC Adv.* **2017**, *7* (22), 13289–13298.

(18) Wang, S.; Ye, J. H.; Han, Z.; Fan, Z.; Wang, C.; Mu, C.; Zhang, W.; He, W. Highly Efficient FRET from Aggregation-Induced Emission to BODIPY Emission Based on Host-Guest Interaction for Mimicking the Light-Harvesting System. *RSC Adv.* **2017**, *7* (57), 36021–36025.

(19) Zhang, J.; Huang, Y.; Wang, D.; Pollard, A. C.; Chen, Z. G.; Egap, E. Triblock Near-Infrared Fluorescent Polymer Semiconductor Nanoparticles for Targeted Imaging. *J. Mater. Chem. C* **2017**, *5* (23), 5685–5692.

(20) Majumdar, P.; Yuan, X.; Li, S.; Le Guennic, B.; Ma, J.; Zhang, C.; Jacquemin, D.; Zhao, J. Cyclometalated Ir(Iii) Complexes with Styryl-BODIPY Ligands Showing

near IR Absorption/Emission: Preparation, Study of Photophysical Properties and Application as Photodynamic/Luminescence Imaging Materials. *J. Mater. Chem. B* **2014**, *2* (19), 2838–2854.

(21)   Lambert, C.; Scherpf, T.; Ceymann, H.; Schmiedel, A.; Holzapfel, M. Coupled Oscillators for Tuning Fluorescence Properties of Squaraine Dyes. *J. Am. Chem. Soc.* **2015**, *137* (10), 3547–3557.

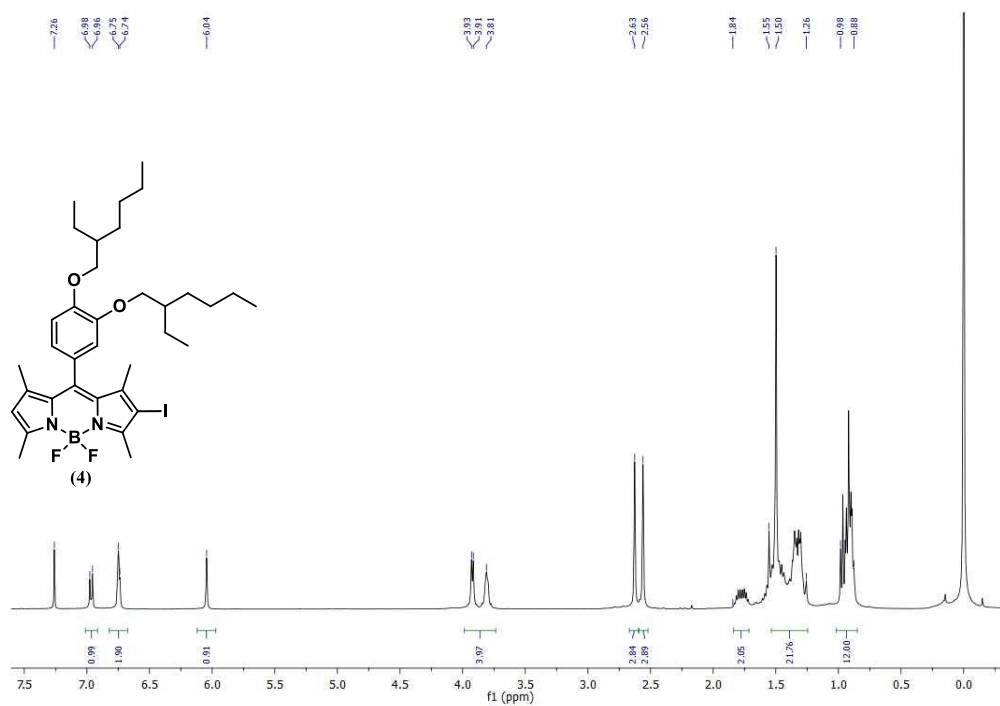**3,4-bis((2-ethylhexyl)oxy)benzaldehyde (1) ^{1}H NMR, CDCl₃**
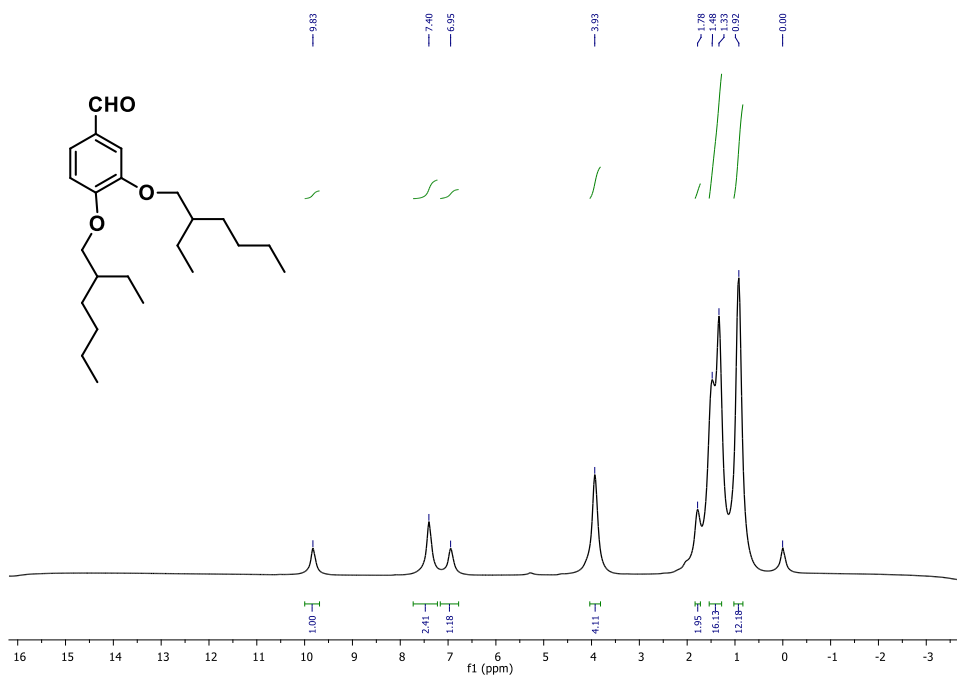
10-(3,4-bis((2-ethylhexyl)oxy)phenyl)-5,5-difluoro-1,3,7,9-tetramethyl-5H-dipyrrolo[1,2-c:2' ,1'-f][1,3,2]diazaboinin-4-ium-5-uide (2) ^{1}H NMR, CDCl₃
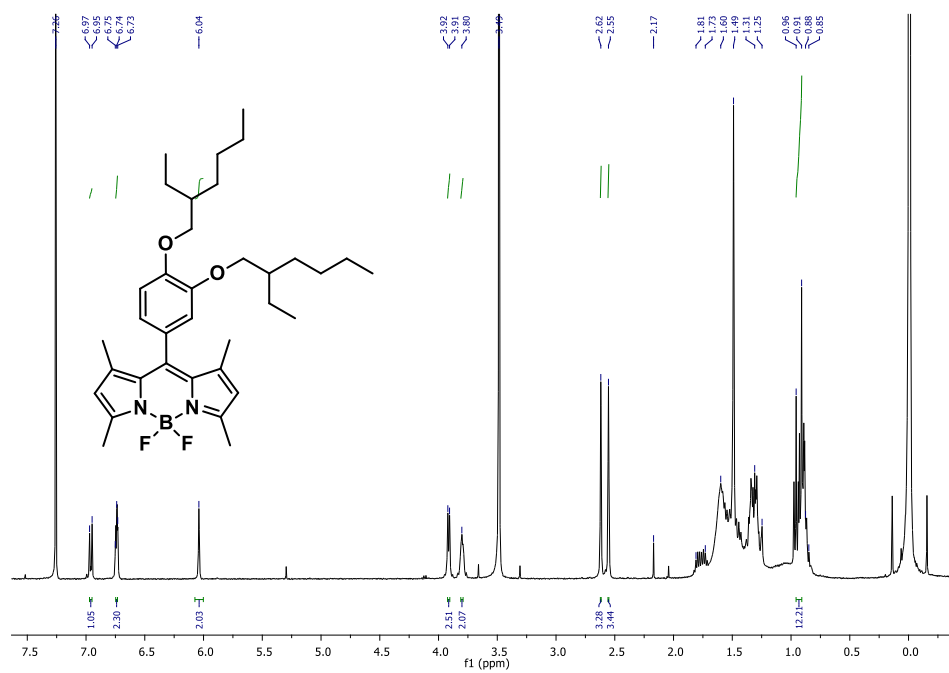
10-(3,4-bis((2-ethylhexyl)oxy)phenyl)-5,5-difluoro-2-iodo-1,3,7,9-tetramethyl-5H-dipyrrolo[1,2-c:2',1'-f][1,3,2]diazaborinin-4-ium-5-uide

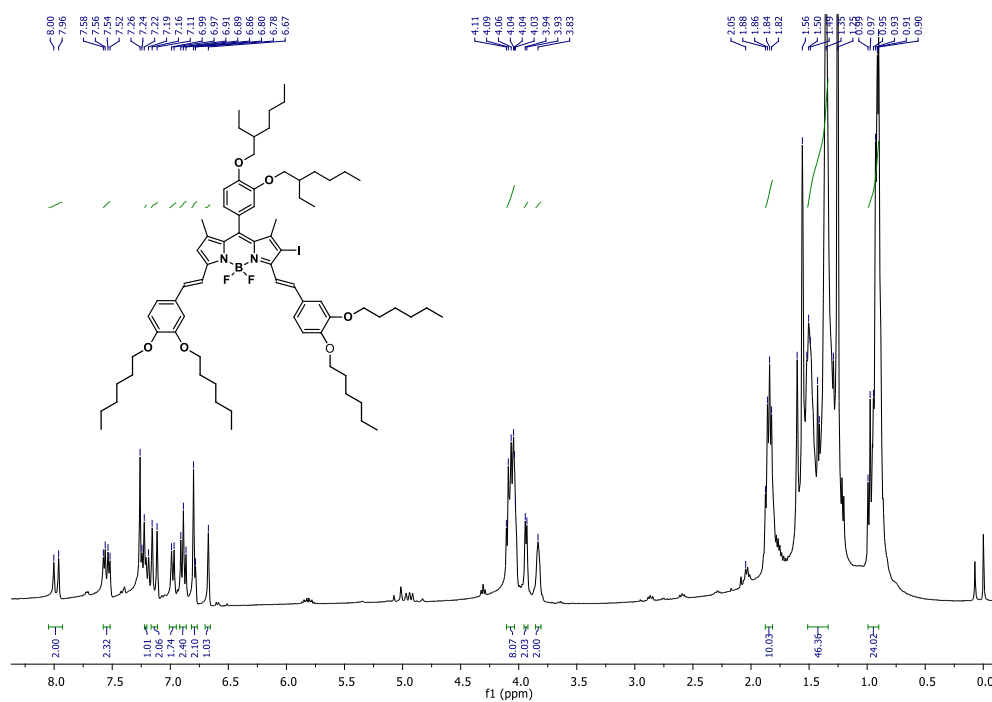**Compound (3) ^{1}H NMR, CDCl$_3$**

Compound (3) ^{13}C NMR, CDCl$_3$
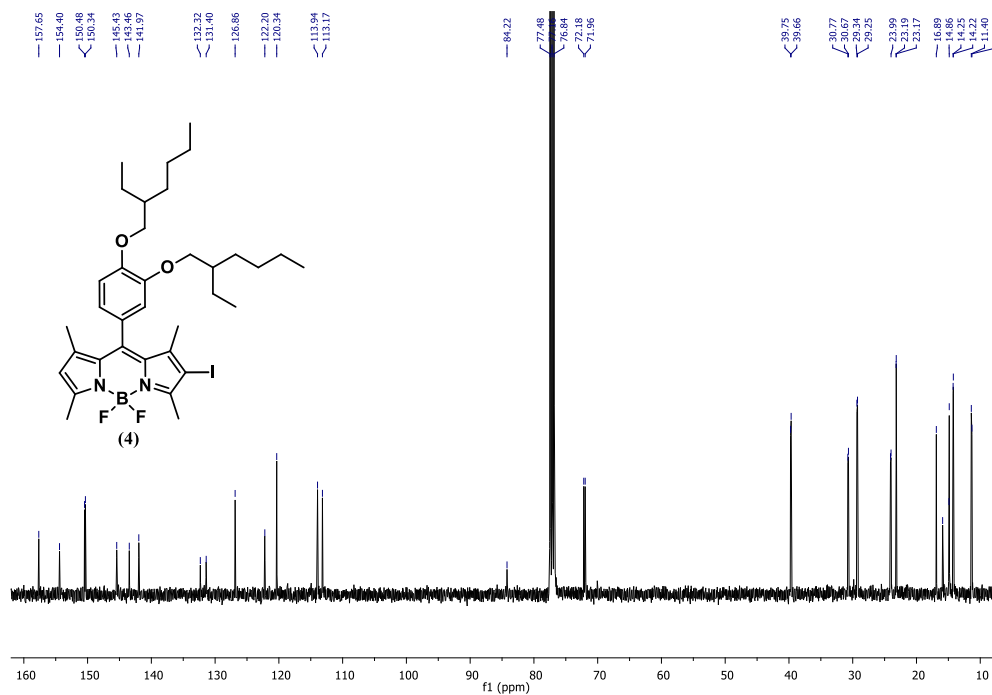
(E)-10-(3,4-bis((2-ethylhexyl)oxy)phenyl)-7-(3,4-bis(hexyloxy)styryl)-5,5-difluoro-2-iodo-1,3,9-trimethyl-5H-dipyrrolo[1,2-c:2',1'-f][1,3,2]diazaborinin-4-ium-5-uide
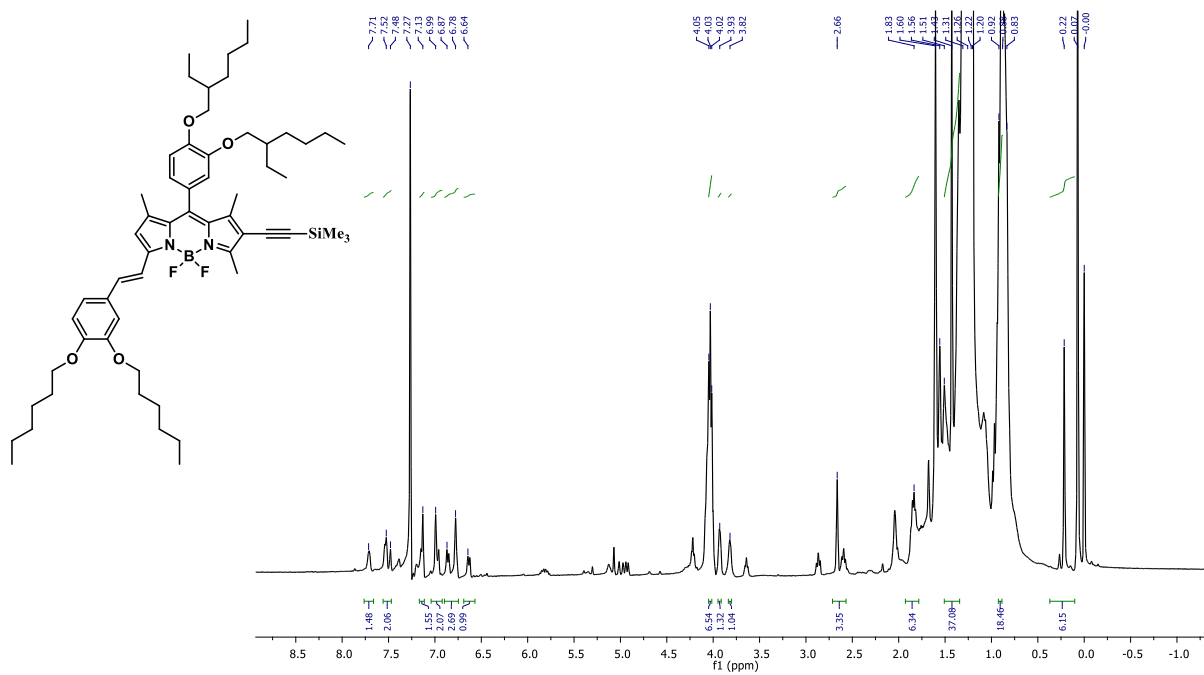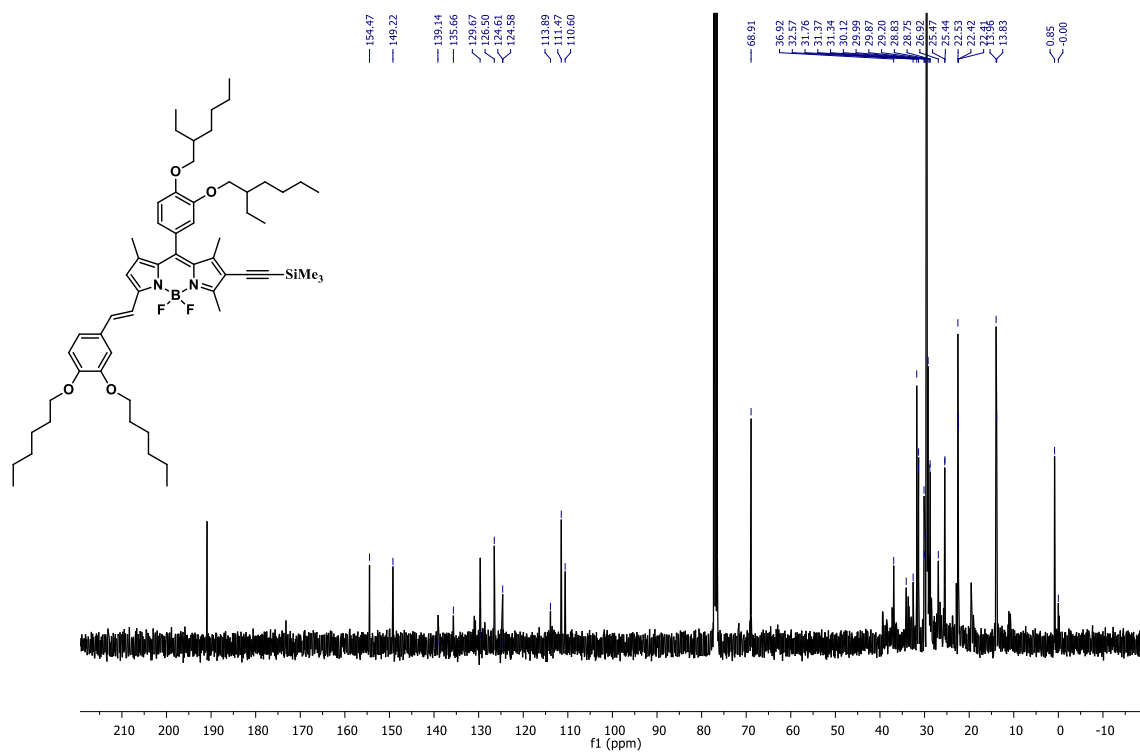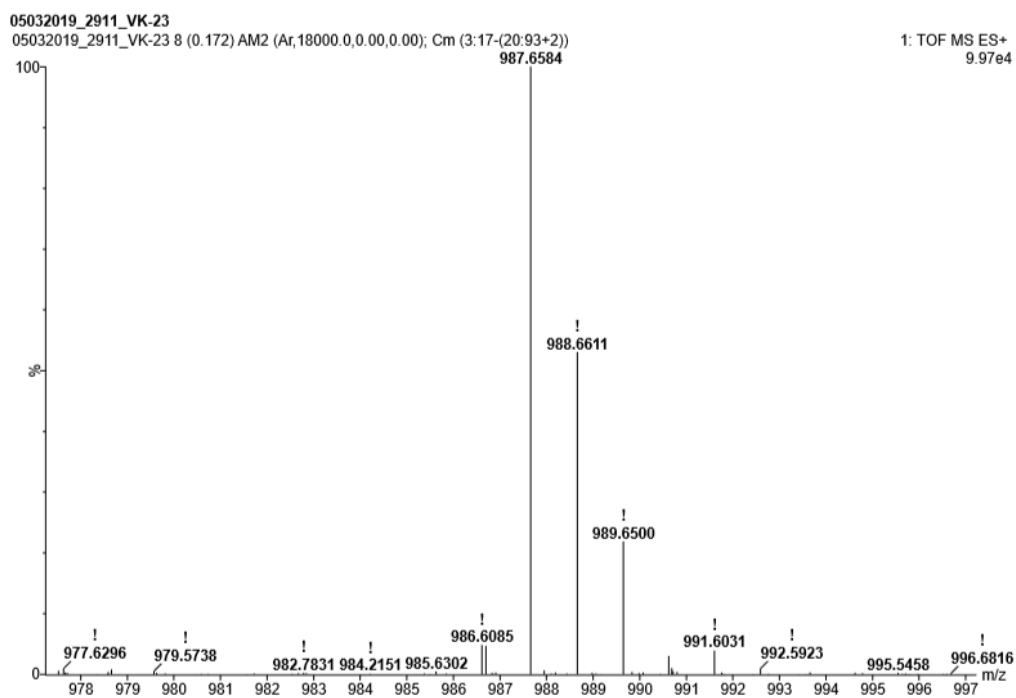
Compound 3a ^{1}H NMR, CDCl$_3$
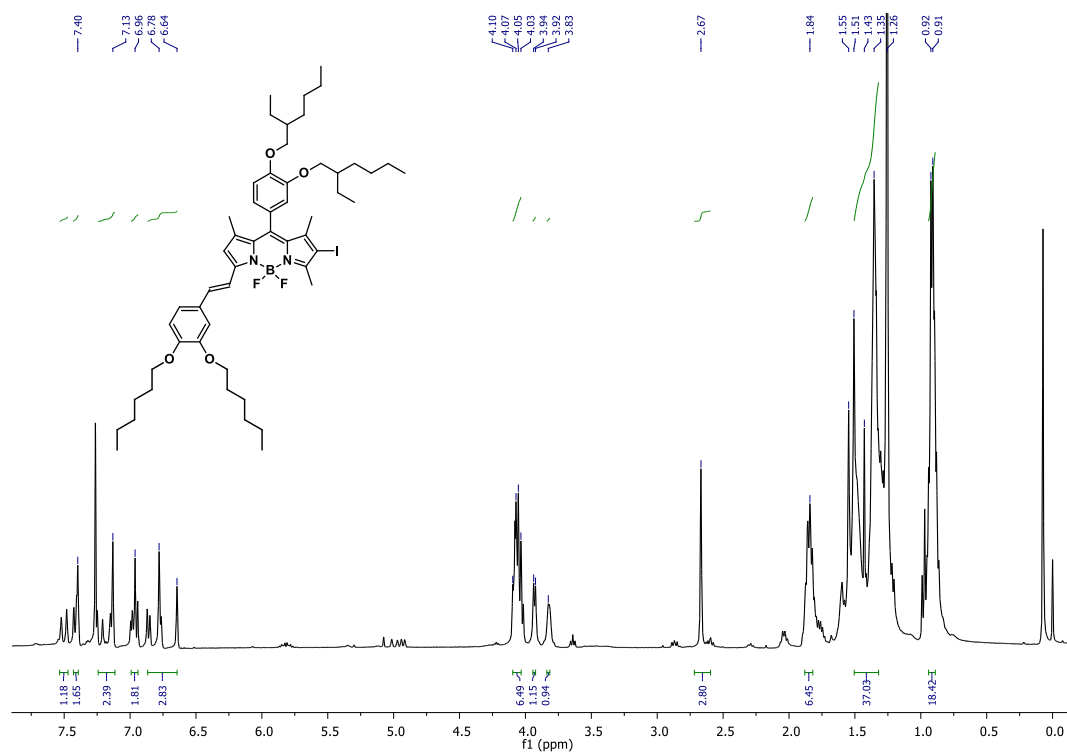
Compound 3a ^{13}C NMR, CDCl$_3$
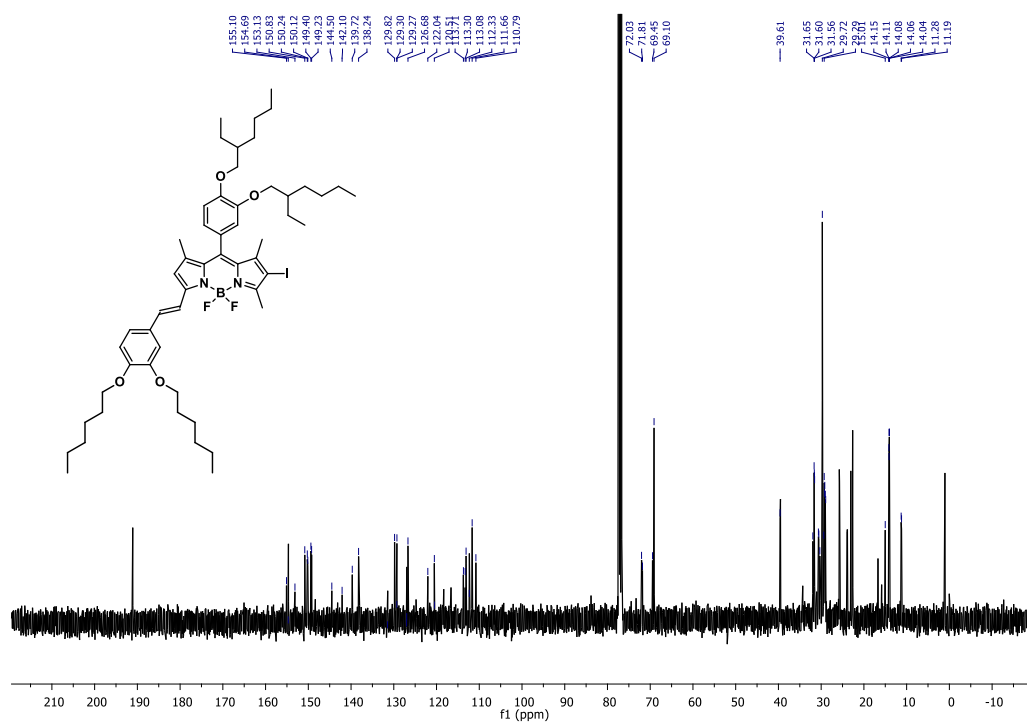
ESI-TOF: Mass Spectroscopy of compound 3a
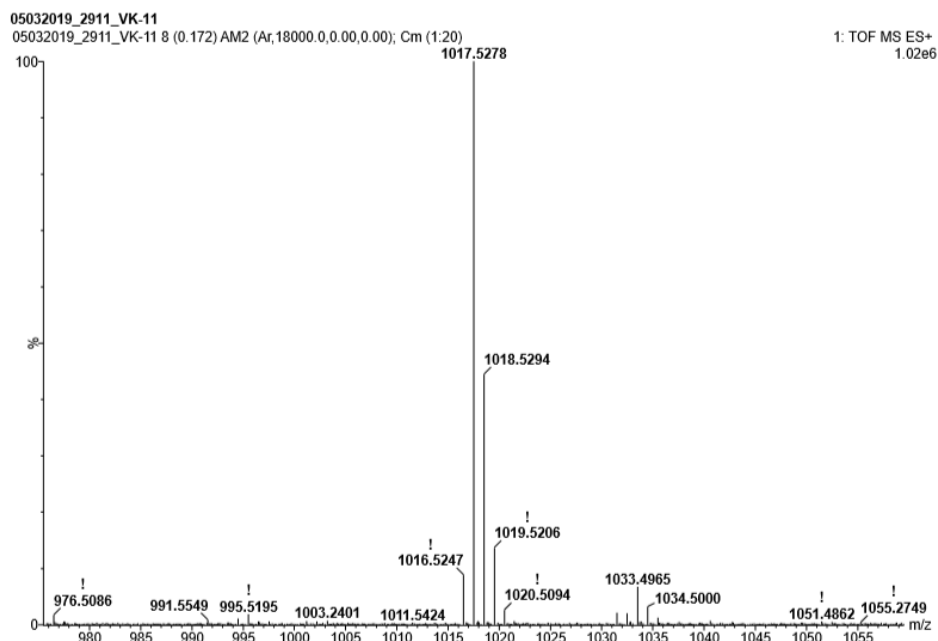
05032019_2911_VK-11
05032019_2911_VK-11 8 (0.172) AM2 (Ar,18000.0,0.00,0.00); Cm (1:20)

1: TOF MS ES+
1.02e6

10-(3,4-bis((2-ethylhexyl)oxy)phenyl)-3,7-bis((E)-3,4-bis(hexyloxy)styryl)-5,5-difluoro-2-iodo-1,9-dimethyl-5H-dipyrrolo[1,2-c:2',1'-f][1,3,2]diazaborinin-4-ium-5-uide

Compound 5a ^{1}H NMR, CDCl₃

¹³C NMR, CDCl₃
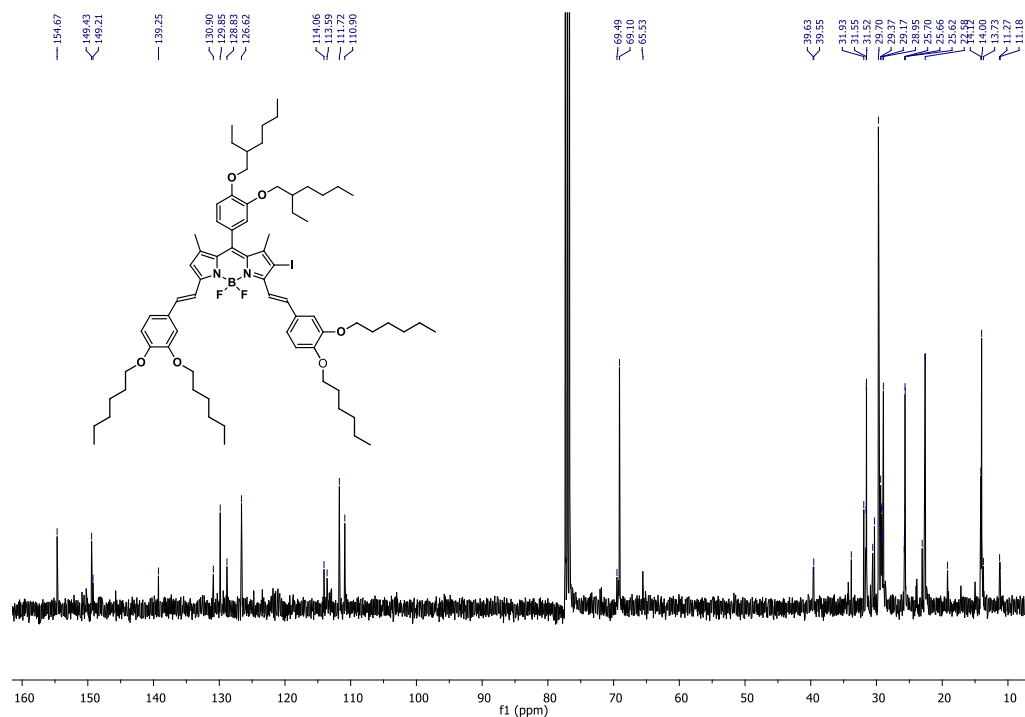
^{13}C NMR, CDCl$_3$

(E)-10-(3,4-bis((2-ethylhexyl)oxy)phenyl)-7-(3,4-bis(hexyloxy)styryl)-5,5-difluoro-1,3,9-trimethyl-2-((trimethylsilyl)ethynyl)-5H-dipyrrolo[1,2-c:2',1'-f][1,3,2]diazaborinin-4-ium-5-uide
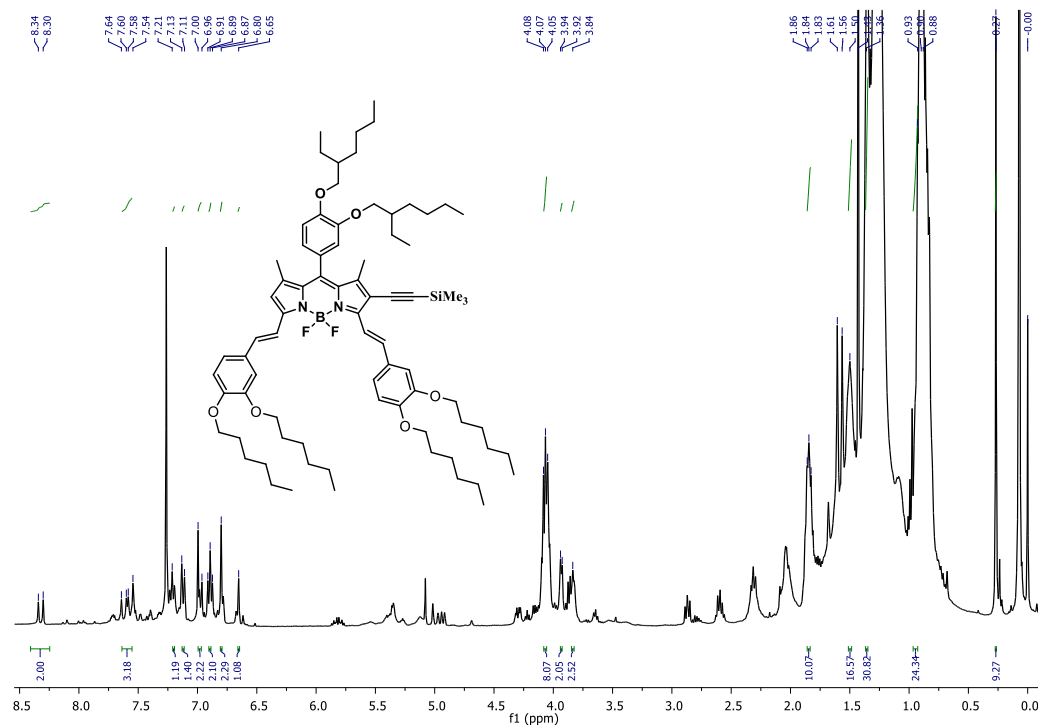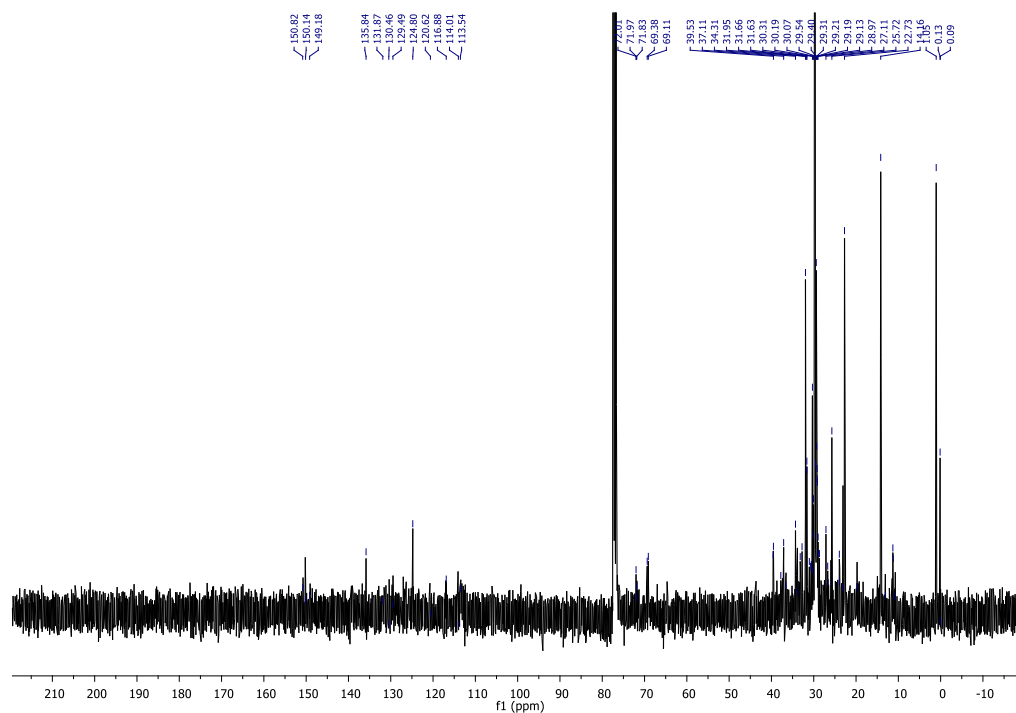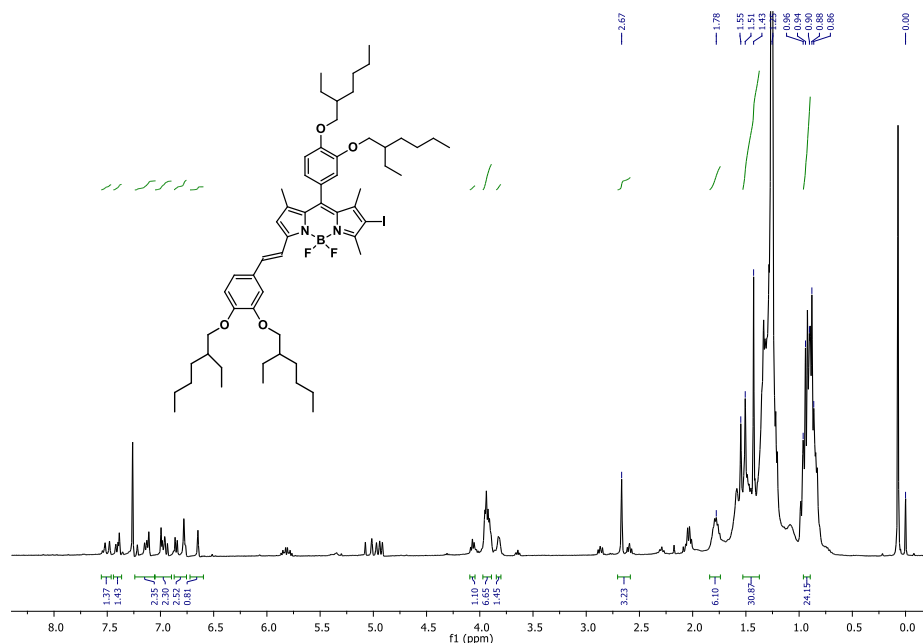
Compound 4a ¹H NMR, CDCl₃

Compound 4a ^{1}H NMR, CDCl$_3$

^{13}C NMR, CDCl$_3$

ESI-TOF: Mass Spectroscopy of compound 5a

10-(3,4-bis((2-ethylhexyl)oxy)phenyl)-3,7-bis((E)-3,4-bis(hexyloxy)styryl)-5,5-difluoro-1,9-dimethyl-2-((trimethylsilyl)ethynyl)-5H-dipyrrolo[1,2-c:2',1'-f][1,3,2]diazaborinin-4-ium-5-uide

Compound 6a ¹H NMR, CDCl₃
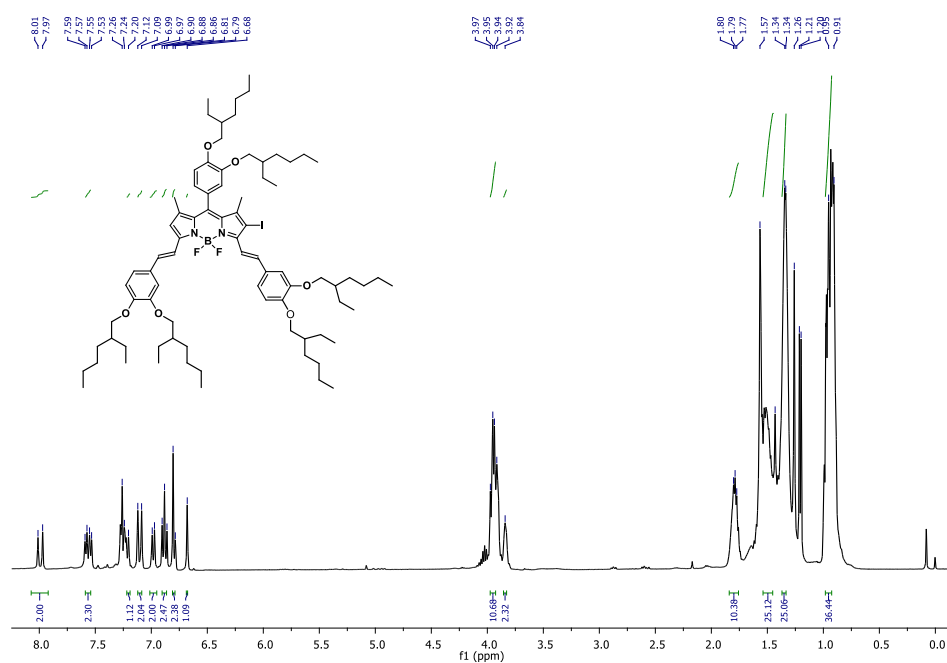
Compound 6a ^{1}H NMR, CDCl$_3$

Compound 6a ¹³C NMR, CDCl₃

Compound 6a ^{13}C NMR, CDCl$_3$

(E)-10-(3,4-bis((2-ethylhexyl)oxy)phenyl)-7-(3,4-bis((2-ethylhexyl)oxy)styryl)-5,5-difluoro-2-iodo-1,3,9-trimethyl-5H-dipyrrolo[1,2-c:2',1'-f][1,3,2]diazaborinin-4-ium-5-uide
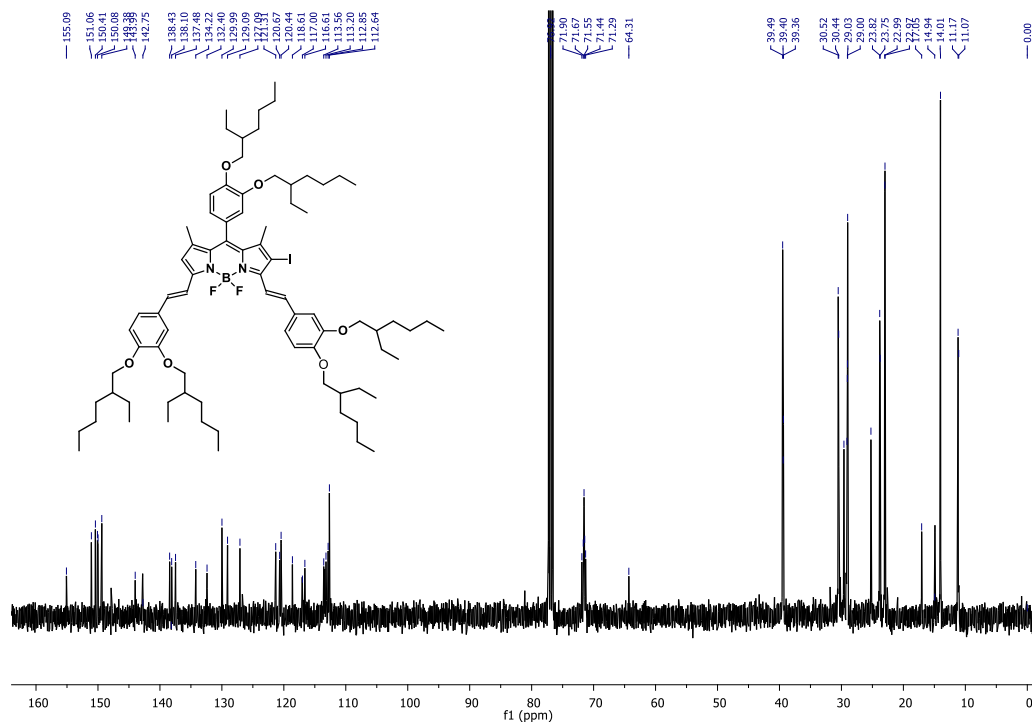
Compound 3b ¹H NMR, CDCl₃

10-(3,4-bis((2-ethylhexyl)oxy)phenyl)-3,7-bis((E)-3,4-bis((2-ethylhexyl)oxy)styryl)-5,5-difluoro-2-iodo-1,9-dimethyl-5H-dipyrrolo[1,2-c:2',1'-f][1,3,2]diazaborinin-4-ium-5-uide
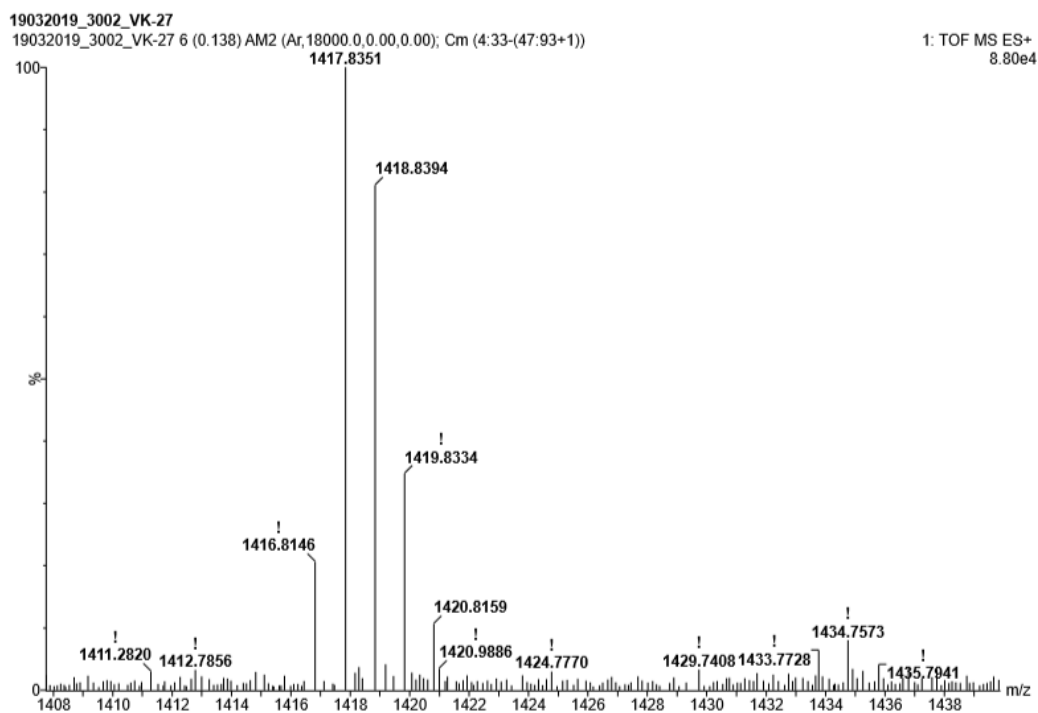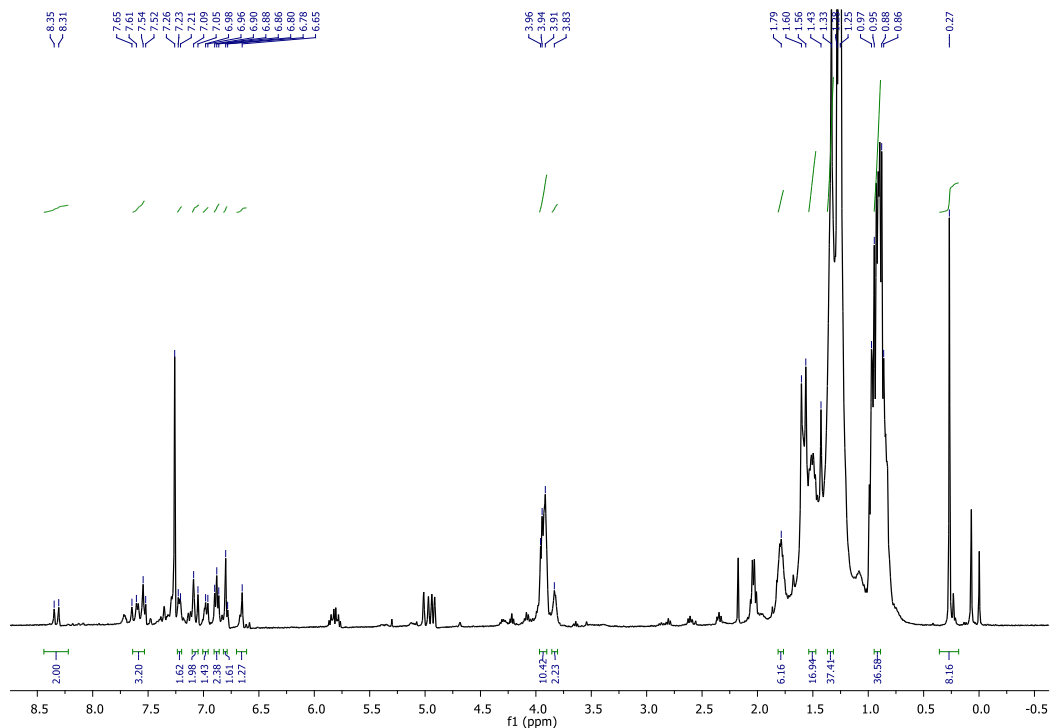
Compound 5b ¹H NMR, CDCl₃

¹³C NMR, CDCl₃

ESI-TOF: Mass Spectroscopy of compound 5b

10-(3,4-bis((2-ethylhexyl)oxy)phenyl)-3,7-bis((E)-3,4-bis((2-ethylhexyl)oxy)styryl)-5,5-difluoro-1,9-dimethyl-2-((trimethylsilyl)ethynyl)-5H-dipyrrolo[1,2-c:2',1'-f][1,3,2]diazaborinin-4-ium-5-uide

Compound 6b ¹H NMR, CDCl₃

ESI-TOF: Mass Spectrum of compound 6b

58